Marie Skłodowska-Curie Actions (MSCA)
Innovative Training Networks (ITN)
H2020-MSCA-ITN-2019

861079 – NextMGT

(Next Generation of Micro Gas Turbines for High Efficiency, Low Emissions and Fuel Flexibility)

Innovation in heat exchanger design for MGTs including energy storage

Deliverable No. 18
D3.2

Summary of
Milestones 8 & 10

Date: 26 June 2022

This project has received funding from the European Union's Horizon 2020 research and innovation programme under Marie Sklodowska-Curie grant agreement No 861079

Contents

1. Introduction

The main objective of work package three (WP3) is to develop innovative methods to enhance aerodynamic, mechanical and electrical aspects of MGTs and utilization of new materials to develop suitable storage systems to enable effective MGT system operation.

Three early-stage researchers (ESRs) are involved in this work package. The section below provides an overview of the ESRs' expected R&D activities within the frame of the project:

WP3: System components innovations and integration with power systems and energy storage

The focus is to investigate innovations in system component design and integration with power systems and energy storage for improved overall performance, increased reliability, reduced cost and flexibility for back-up of intermittent renewables.

ESR10 (CITY) will be concerned with the optimisation of the whole electrical system, consisting of power electronics, high-speed electrical generator and the control system. The aim of the research is to investigate innovative configurations that will significantly reduce the size and cost of the electrical unit, whilst achieving a high overall electrical efficiency (> 95%).

ESR11 (AUTH) will investigate the use of compressed metal foam to enhance the heat transfer efficiency in compact heat exchangers and new CMCs in advanced MGT systems. In addition to developing suitable design and optimisation methods for heat exchangers, this project will explore cost and environmental compatibility of next generation materials for the next generation MGT systems.

ESR12 (UNIGE) will study high temperature energy storage solutions for MGT systems as well as electrochemical storage technologies and the requirements for effective integration with MGTs in applications such as CSP. The output from this ESR will be an optimised management strategy for the MGT-energy storage system, considering both cost and efficiency.

Ultimately, when the innovations are brought together into a single system, the cumulative effect will be to achieve the desired step change in MGT technology.

The tasks, deliverables and milestones of the current periodic reporting are mainly focusing on state-of-the-art studies carried out by the ESRs. However, preliminary results from modelling and experimental work have also been reported in the report. This report focuses on the work done by both ESR11 and ESR12.

Part 1 relates to the work provided by ESR11 at AUTH which completes the deliverable on the state of the art of "innovations in heat exchanger design for MGTs". The achievement of the milestone "Definition of methods of analysis of heat transfer performance of metallic foams" is summarised in Section 4.

Part 2 relates to the work provided by ESR12 at UNIGE which completes the section of the mentioned deliverable "including energy storage". The achievement of the milestone of the "Validation of the MGT model with experimental results (Validation of a T100 Transient Model with Injection of Compressed Air) is outlined in Section 7.

Part 1

2. Overview of Work by ESR11

2.1 Scope

The use of compact heat exchangers has become very attractive in aerospace, automotive, and power generation applications. The need for decentralised power generation is increasing over the past decades targeting a significant level of energy saving. An attractive solution within this market is the power generation and propulsion through micro gas turbines. A micro-GT is considered a compact gas turbine, generating power at about 500 kW or below, in a Brayton cycle. It consists of a compressor and a turbine running on a single shaft, a combustion chamber, and a generator. Recuperator is an optional component that is employed to achieve an adequate thermodynamic efficiency [1]. Such turbines have lower thermal efficiency than higher power gas turbines. The usual pressure ratio is between 3-4 while thermal efficiency rises from about 20% without a recuperator to 30% with the presence of recuperator respectively assuming a recuperator of at least 87% effectiveness [2]. Although the thermal efficiency of reciprocating engines ranges from 35-40%, the emissions of CO and NOx are higher than those of micro-GT. Recuperators are costly to a great extent, in maintenance, materials, and manufacturing. Higher performance demands the increase of heat exchanger area, increasing the manufacturing cost such as machining, welding, and brazing. The recuperator accounts for 25-30% of the overall cost of the system [3]. Apart from recuperators, the thermal management for micro-GT increased efficiency can also be achieved using intercoolers and cooling-air coolers [1]. To meet the cost requirements the system must be kept as simple as possible, including a high-performance recuperator [4]. The packaging must also be compact. The annular wrap around arrangement consists of a cylindrical shaped recuperator with the main parts in the internal diameter inside it (Figure 2-1). A different arrangement may have the recuperator at the rear side of the turbomachinery.

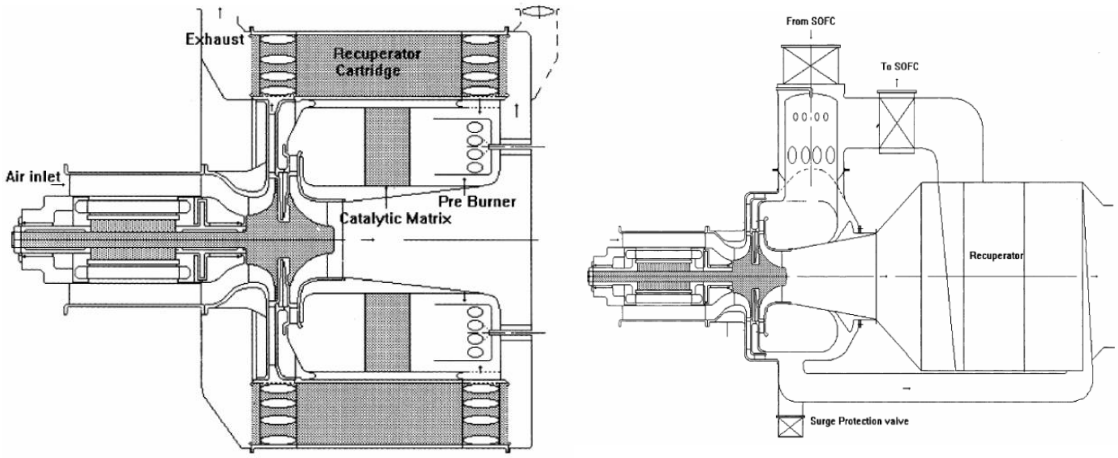

Figure 2-1: Micro-GT system with recuperator developed by C. Rogers ITC a) annular wrap-around recuperator, b) rear-mounted recuperator [1].

Well established companies all around the world have invested successfully in micro-GT and still have the potential to increase claim to the energy market for distributed power. The most popular companies are Honeywell, Capstone, Ingersoll-Rand, Elliott, Allison, Teledyne in USA, Volvo, ABB, Aurelia Turbines, Bowman, Turbec in Europe, and Toyota, Ebara, Kawasaki, Nissan, IHI in Japan. These companies focus on recuperators as the best choice to increase thermal efficiency in micro-GTs [5].
The recuperated Brayton cycle uses gases leaving the turbine and entering the recuperator, transferring heat to the compressed air that comes out of the compressor. Then the preheated air enters the combustor. The mixture in this case needs less fuel to reach the required turbine inlet temperature and increases the thermal efficiency. In addition to the lower fuel consumption, the recuperator also contributes to a lower noise level in aerospace applications [6].

Apart from the benefits, there are challenges that need to be addressed. This intervention to the cycle reduces the designed pressure ratio depending on the recuperator geometry, surface type, connections, and fluid velocity. This issue can be partially addressed adjusting design parameters and design point, but it cannot be fully eliminated. There are also other important parameters to consider. Proper installation, operation and maintenance require the combination of multiple disciplines of engineering such as fluid mechanics, stress analysis, materials and processes, and machining. The recuperators are heat exchangers that can be considered pressure vessels. The pressure ratio in a micro-GT is much lower than larger scale gas turbines. Therefore, in the current study mechanical issues caused by the pressure will not be examined. However, proper handling, packaging, and installation are required to avoid mechanical damage. The process of installation, operation, and maintenance shall be carried out according to the manufacturer specification because it can affect the effectiveness, pressure drop, lifetime, service time and as a result the total cost. During operation, the heat exchanger is subject to fouling depending on the conditions. Fouling increases the thermal resistance of the surfaces and affects the overall heat transfer coefficient hence, the effectiveness [7]. Although measures shall be taken to reduce fouling, heat exchanger cleaning shall be planned regularly as a part of maintenance process [8]. Extra care should be taken for the leakages that can occur due to defects in the walls, connections, welding, and brazing areas. Through welding process flow passages can be formed and leakages and fluid mixing may be prevented. Advanced sealing quality, proper use and regular maintenance can also eliminate leaking and mixing issues.

Typical materials used for recuperators are: Stainless steel 300 series (AISI 307 SS and 347 SS) for temperatures below 675 °C, and Inconel 625, Inconel 803, Haynes 120, Haynes 214 and PM2000 up to 900 °C. Despite its better performance, Inconel is not the most preferable material due to the prohibitive cost. Cost requirements and the need for turbine inlet temperature increase have mandated the use of ceramic materials in micro gas turbine components [9]. Several approaches have been proposed for SiC components in micro-GT with ongoing progress on heat exchangers development [10] (Figure 2-2). Early developments of ceramic heat exchangers include prime surface, plate-fin, and tubular configurations [4, 11]. An effort to manufacture micro-GT rated up to 100kW with efficiencies above 40% led to the conclusion that all the components after the combustor should be ceramic to withstand the high turbine inlet temperatures [12].

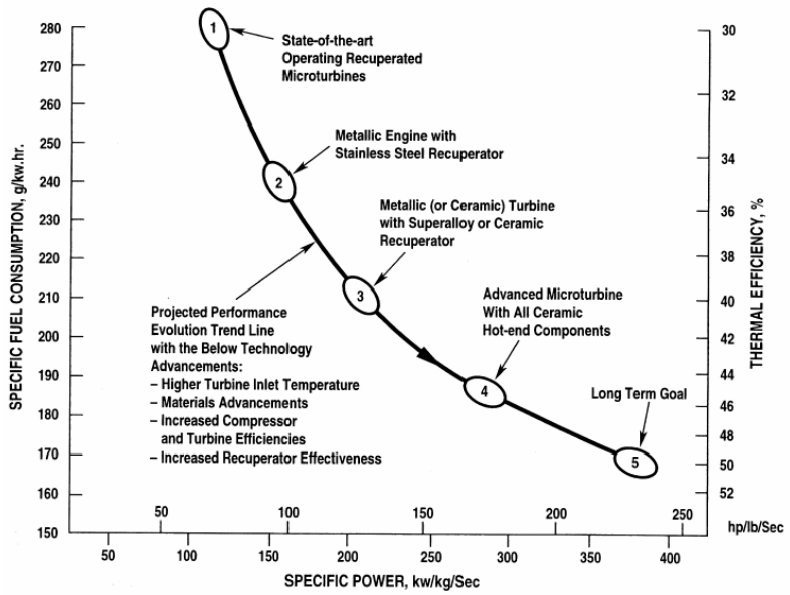

Figure 2-2: Projected performance evolution for recuperated micro-GT [10].

As a material which is manufactured by homogenous diffusion of gas state in a solid metal phase, porous materials constitute a well promising solution for thermal management of micro-GTs [13] [14]. The most commercially available metal foams are made of Aluminium, Copper, Nickel, and metal alloys [15]. There is a big trend in the development of Inconel types as well as ceramic materials due to higher performance requirements for heat exchangers. Foams are categorised depending on the

material, cell topology or manufacturing process. Regarding cell topology, there are open cell foams, where the pores are connected or closed cell foams, where the pores are not connected. Open-cell metal foams are a type of porous materials that combine low density and notable properties in thermal storage and heat transfer, as well as mechanical and acoustic properties [16, 17, 18]. The high specific area, reduces volume, weight and enhances compactness which ranges from 500 to over 10,000 m^2/m^3. High porosity materials are quite common in these applications. High porosity (above 90%) ensures high fluid permeability and even lower weight. Metal or ceramic foams hold great promise for a variety of applications, many of those with lightweight requirements. The most common applications that require these properties are catalysts, filters, and applications that need heat and mass transfer [19]. This material combines high strength over density and high fracture toughness needed for weight critical applications. The open cell bodies can offer high thermal conductivity combined with convection increasing the heat transfer potential. The tortuosity of the material allows the excellent fluid mixing. The structure can give good energy absorption, excellent resistance to thermal shock, thermal cycling as well as noise attenuation [20, 21, 22].

2.2 Motivation

The market of micro-GT currently lacks innovation in design and materials selection of the micro-GT components but has a good potential to grow fast in multiple industrial applications. The main requirement shall focus on new designs of micro-GT components, alternative fuels as well as combined cycles for maximised performance and reduced carbon footprint. Combined cycles can increase the efficiency but also increase the cost, weight, and volume of the system. An approach that has achieved significantly higher efficiency, is the use of heat exchanger in micro-GT as a recuperator. However, a current micro-GT with high performance is expensive due to the excessive cost of materials, manufacturing, and maintenance of the heat exchanger [23]. Over the last 40 years, the evolution of recuperators from bulky components has led to recent lightweight units and the secondary surfaces have been limited to primary surface types. The effectiveness starts from about 85% and can reach 90% if volume and weight constraints are not considered. Apart from the high performance and low cost, these applications require weight and volume reduction due to packaging, handling, and equipment footprint constraints. Especially in aerospace industry weight reduction is of utmost importance for additional fuel savings [24, 25]. Current goals are to investigate the effect of the use of novel materials and surface types in the heat exchanger performance and as a result in the overall performance of the micro-GT. Metal and ceramic foams are already known for their exceptional properties and are widespread in the market for several applications. However, they have not debuted in the micro-GT market and their use is still not fully investigated in this application. Consequently, a significant gap exists in the effect of the foam incorporation to the overall performance of micro-gas turbine.

2.3 Aim and Objectives

The aim of the current report is to review the state of the art of innovation in design of compact heat exchangers that can be used as recuperators in micro-GT. This report summarises the distinct types of recuperators and the recent advancements in industrial applications. Smart solutions for compactness increase and heat transfer enhancement are investigated. A brief description of the materials and manufacturing methods is given to evaluate the potential for further thermal efficiency improvement.
The aim of the overall work of ESR11 is the development of a heat exchanger for the application of micro gas turbine systems. Implementation of this concept is conducted through heat transfer and pressure drop model methodology capable of predicting the influence of geometrical characteristics of the heat exchanger on component and system level performance. To achieve this, the following objectives shall be met:

- Investigation of methods of analysis of heat transfer performance and pressure drop of porous media.
- Design optimisation of a heat exchanger through mathematical modelling.
- Design optimisation of a heat exchanger through computational simulations.
- Evaluation of selected methods through experimental verification of generated results.

3. Innovation in Compact Heat Exchangers

3.1 Performance Requirements and Capabilities of the Main Types of Heat Exchangers

The last two decades new types of small size and compact recuperators have been proposed for micro-GT applications. The compact definition refers to surface area densities above 200 m^2/m^3 and low hydraulic diameters. However, the investigation of heat transfer geometries has been carried out over the last 70 years [2]. The usual fluids in recuperator applications are compressed air and exhaust gas. These fluids share similar values of mass flow rate and properties such as viscosity specific heat capacity and density. Therefore, the heat capacity rate ratio is considered equal to 1. There are flow arrangements in recuperators like parallel, counterflow, crossflow and combinations of them. High recuperator effectiveness must be achieved by counterflow type. These heat exchangers can be classified into three categories depending on the heat transfer surface geometry: primary surface (PSHE), plate-fin (PFHE), and tubular shaped heat exchangers.

Plate-fin and primary surface recuperators can achieve high effectiveness [26]. Despite the high effectiveness in these two types, high surface area increases the process cost, as the assembly requires more welding or brazing. Primary surface recuperators are becoming more popular to many gas turbine manufacturers since their effectiveness reaches up to 90% when the pressure loss is only 5%. It is stated that for a given thermal load the required unit volume for plate-fin and tubular recuperator is 2.8 and 11.8 times greater than primary surface types [27]. PFHE and tubular types can take advantage of the fins or baffles as structural elements for mechanical integrity besides thermal enhancement [28]. On the other hand, high-pressure passages of primary surfaces may undergo high strain under exposure to high temperature creep conditions [29]. Plate-fin recuperators with high effectiveness introduce extra weight in the component, so they are not recommended for lightweight applications [26].

Major design criteria include compatibility to micro-GT performance, relative low mass flow rate, high heat transfer effectiveness, low to moderate pressure containing capability, and low pressure drop. The recuperator shall also have thermal stability, resistance to thermal cycling, and corrosion resistance. Lifetime goal shall be 50,000 hours for micro-GT generator sets. Additional important requirements are high reliability and compact and lightweight matrix. With regards to fabrication, the need for furnace brazing must be minimum and most sealing surfaces shall be bonded via welding. Automation is of paramount importance for flexibility from low to high volume production. The number of matrix parts should be kept minimum to reduce process time and cost but at the same time the surface compactness should be high. In terms of cost, the manufacturing companies aim to zero scrap, minimum labour time and the goal for unit cost is not to exceed 1.5 times the material cost. Installation must be taken into consideration focusing on simplicity. Therefore, hydraulic compatibility with micro-GT is imperative to ease the installation. Maintenance considerations shall include easy replacement of the recuperator or individual components, easy detection of leakages and easy repair of weldments. An important advantage would be the adaptability to future growth performance. This can be higher temperature variations, retrofit capability and flexibility to new materials [30, 10].

3.2 Design Innovation in Compact Heat Exchangers

3.2.1 Primary Surface Heat Exchangers (PSHE)

The main characteristic of this group is that heat transfer surface geometry is 100% effective without the contribution of secondary surfaces with fin efficiency effects [8]. They are normally formed by stacked corrugated plates. There is usually a lack of supporting elements between flow passages rendering this type more beneficial for low pressure ratio applications [28]. Nowadays flow passages can be formed by welding applications replacing gradually the long and elevated temperature process of brazing, withstanding higher differential pressures [2]. Plates patterns are categorised in three types: cross-corrugated (CC), corrugated-undulated (CU), and cross-wavy (CW) [31].

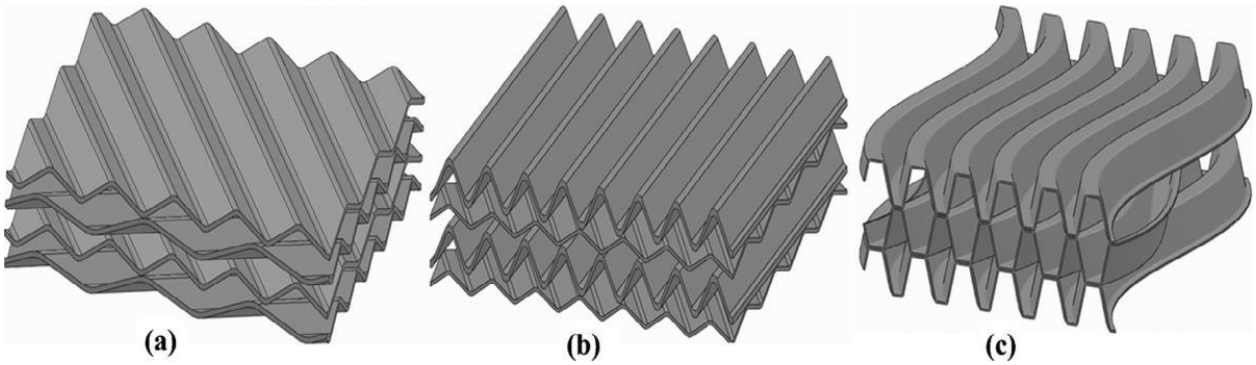

Figure 3-1: Main patterns of plates a) cross-corrugated (CC) surface, (b) corrugated-undulated (CU) surface, (c) and cross-wavy surface [31].

A representative example of this type of heat exchanger is developed by RSAB [32]. It is a recuperator made of stainless-steel plates in a CC pattern, completely welded at the edge of each cell. The flow type is counterflow where the air flows through the manifold and is distributed through the channels of the plates, as shown in Figure 3-2a. A PSHE is developed by Ingersoll Rand for similar applications [33]. According to the manufacturer, this recuperator is characterised by its tolerance to high thermal gradients during transient state conditions. Honeywell Corporation developed a PSHE which has welded plates in a CC configuration [2]. An example of plate heat exchanger is included in a 7.5 kW demonstrator which involves ceramic radial flow turbine, combustor, and recuperator (Figure 3-3b) [12]. This is a microchannel recuperator manufactured utilising the process of Laminated Object Manufacturing (LOM) methods. The use of SiC increased the turbine inlet temperature to 1170 °C in this recuperator with effectiveness value of 92% and raised the engine thermal efficiency at the order of 30%. A similar plate type microchannel recuperator was designed by Wilson et al [34]. The inlet temperature of hot gases could reach up to 955 °C with SiC and the overall electrical efficiency could be improved from 27% to over 40%.

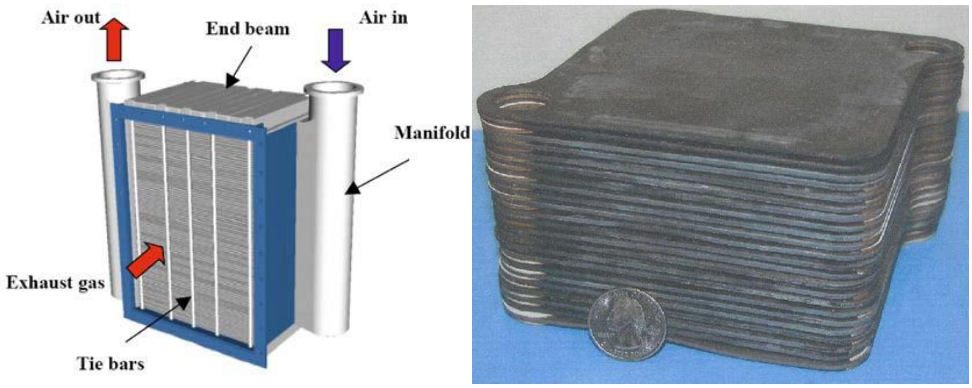

Figure 3-2: Rectangular shape PSHE examples, (a) RSAB recuperator [32], (b) and Ceramic micro-channel gas turbine recuperator module [12].

There are also PSHE with annular shape utilised in micro-GT in a wraparound configuration. The recuperator in Figure 3-3 is used since 1998 by Capstone Turbine Corporation in commercially produced recuperated micro-GT. It consists of hundreds of air cells fabricated by welded steel sheets. High inlet gas temperatures of 850 °C are achieved by this application. Other benefits are simplicity, compactness, and minimal ducting. [35]. Another annular shape primary surface recuperator, presented in Figure 3-4, was developed by ACTE [36]. The annular shape is created by winding a pair of plates in a mandrel. The pair of plates has a CC pattern and is laser welded at the sides for flow separation. There are many contact points all over the body created via laser welding. This pattern mixes the flow generating turbulence for heat transfer enhancement. Bonding at multiple contact points between plates enhance the structural stability which makes this recuperator more suitable for higher operating pressure applications. The flow type is separated in cross flow and counterflow zones. The materials are usually stainless steel and Inconel. There are manufacturing limitations for Inconel because the high modulus of elasticity does not aid the forming process, so thinner sheets of Inconel are recommended for this

design of recuperator. Swiss-Roll annular shape counter flow recuperator is depicted in Figure 3-5 [5]. It consists of a pair of stainless steel-304 plates spirally wrapped around each other. Experimental results proved that the fuel consumption without recuperator is about 1.5 times more than an engine with Swill-Roll recuperator. Numerical results showed that the increase of number of turns from 4 to 8 increased the heat recovery efficiency from 43% to 75%. However, the pressure drop increased from 5% to 19.4%.

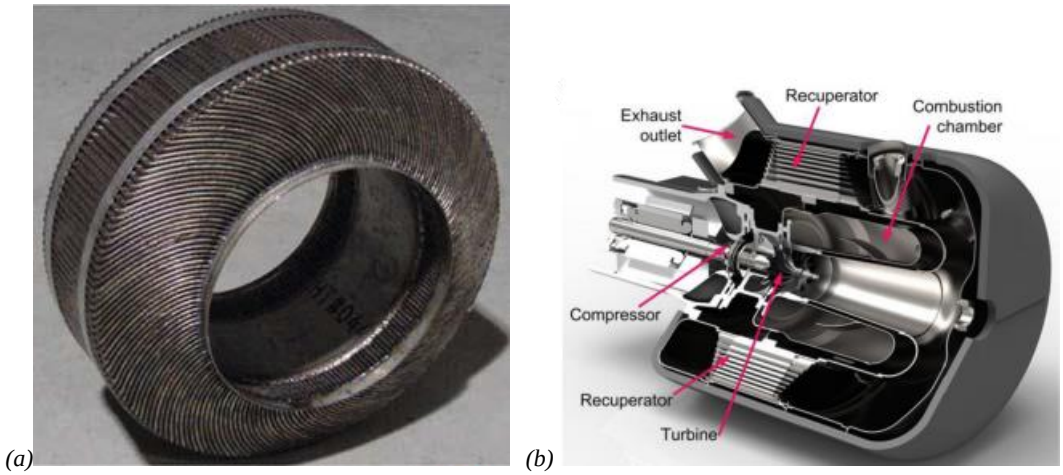

Figure 3-3: Capstone recuperator (a) annular shape, (b) integration to micro-GT [35].

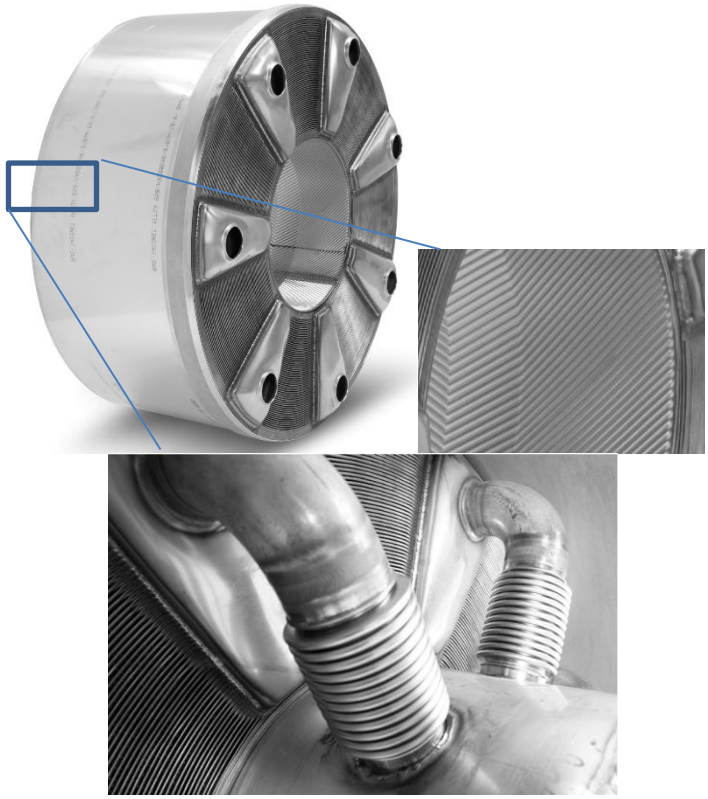

Figure 3-4: Annular recuperator (courtesy ACTE).

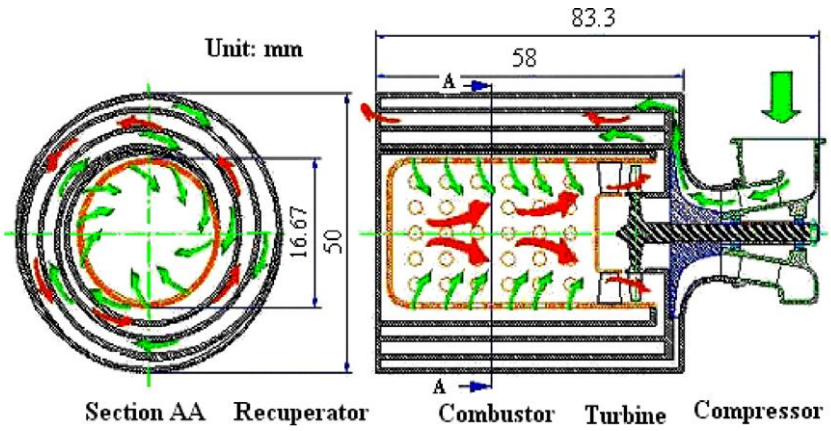

Figure 3-5: The engine with Swiss-Roll recuperator [5].

Printed circuit heat exchangers have been introduced in the market for the use as recuperators due to the low capital cost compared to a conventional heat exchanger. PCHE can achieve approximately 98% effectiveness. They have also been investigated as components in supercritical CO_2 power plants [37, 38] optimizing the design of PCHE for improved cycle efficiency. Numerical simulations showed that the effectiveness reached more than 99% and pressure drop less than 1%. PCHE are considered compact and additionally can operate in high pressures up to 900 bar [39]. Manufactured first in the UK by Heatric Ltd, they consist of plates bonded together and micro channels as fluid passages (Figure 3-6). The channels which are usually semi-circular have very low hydraulic diameters between 1.5 and 3 mm. The channel profile can be straight, wavy, S-shaped fin or airfoil-finned depending on the application requirements [40, 41, 42]. Research has shown that zig-zag shape provides better heat transfer performance than s-shape, while airfoil finned channels show similar thermal performance to zig-zag PCHE but better hydraulic performance [40, 43]. The plates can form simple cross flow and counter flow, or a combination of them [8]. The surface of PCHE is treated as primary because the calculated fin efficiency is remarkably high. Hence, the surface is taken as unity in design calculations. The porosity of this type heat exchanger is lower than plate-fin type. As a result, PCHE are normally heavier for similar hydraulic diameters.

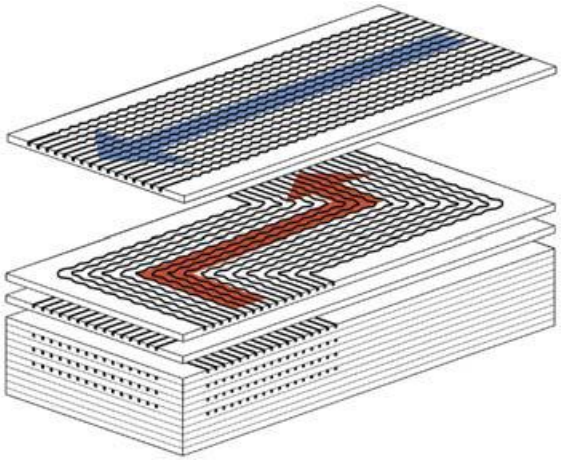

Figure 3-6: Example schematic of PCHE [41]

3.2.2 Plate-Fin Heat Exchangers (PFHE)

This category is characterised by the presence of secondary surfaces with the form of fin structures. The secondary surfaces contribute to the heat transfer surface geometry enhancement. Thus, these structures increase the compactness of the heat exchanger, and decrease the hydraulic diameter. PFHE are recommended for applications where the heat is transferred between a liquid and a gas phase. The low viscosity and low thermal conductivity gas stream should flow on the finned channels to balance the thermal resistances of the liquid and gas sides [8].
A recuperator with design similarities as the RSAB external shape was used for intercooled micro-GT.

However, the main difference is the presence of offset fins (Figure 3-7) [44]. A micro-GT recuperator in spiral configuration and counterflow type was developed at Rolls Royce [45]. The air channels have dimples on metal sheets, and the gas side has perforated extended fins with hydraulic diameters of 1.5 mm and 2.3 mm, respectively. The thermal contact between the fins and the primary surface is not based on any bonding, for thermal gradient reduction and cycling stress relief. This contact is accomplished by the high-pressure air side acting on the plates at each side of the fins. An excellent early development of a compact plate-fin ceramic recuperator by Allied/Signal (Figure 3-9) was intended for the use of cruise-missile applications [11].

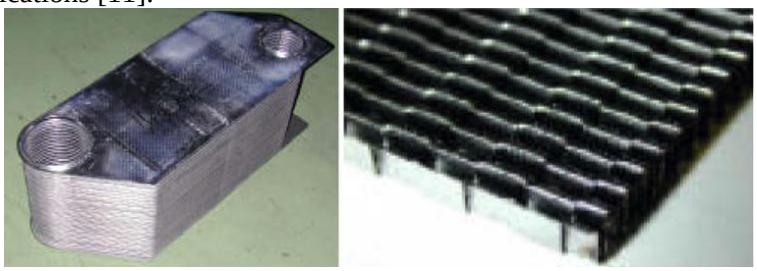

Figure 3-7: PFHE used in intercooled engine [44].

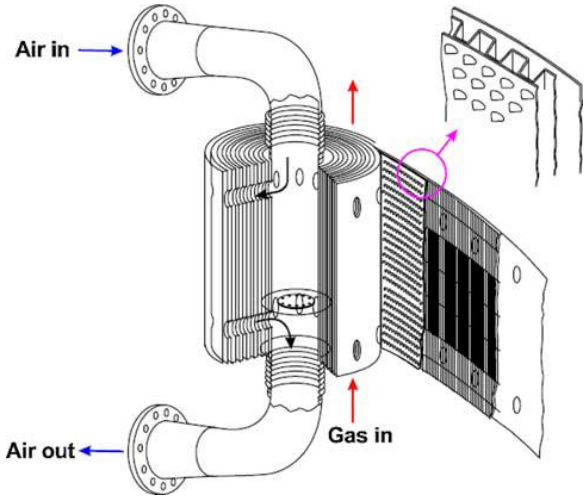

Figure 3-8: Spiral recuperator developed by Rolls Royce for micro-GT [45].

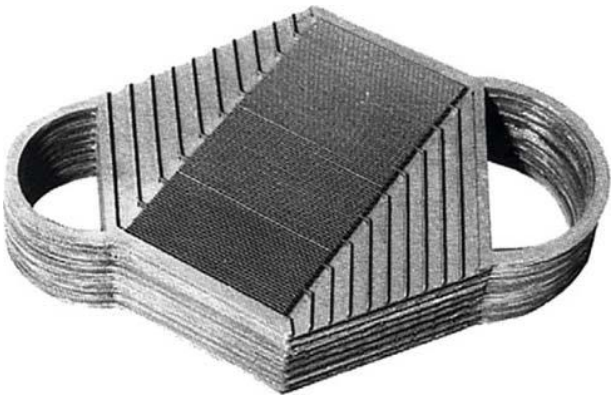

Figure 3-9: Ceramic plate-fin recuperator fabricated by Allied/Signal [11]

3.2.3 Tube Shaped Heat Exchangers

Tubular heat exchangers are mainly used for structural integrity reasons. The compact geometry consists of small hydraulic diameter tubes in several profiles (Figure 3-10) [1]. Elliptical shape is preferred over circular due to the increased heat transfer area and better hydraulic and structural performance. Although this category is known to have excessive cost due to automation requirements for manufacturing [46], high-pressure retaining capability make this this type of heat exchangers

suitable for high pressure turbofan aeroengines. Such type has been developed by MTU for intercooled recuperated aeroengine (IRA) working on VITAL and NEW AC, FP6 research programs focusing on intercoolers for CO_2 propulsion efficiency and reduction in CO_2 and NO_x emissions respectively [47]. Figure 3-11 presents an MTU recuperator with the bundle of profile tubes made of INCONEL alloy 625. This is a two-pass cross-counterflow tube recuperator. Findings from structural analysis have shown that the shape and material offer high performance in terms of Low Cycle- Fatigue (LCF), creep and vibration [48]. Computational Fluid Dynamics (CFD) studies investigated the pressure drop minimisation via changing operating conditions [49]. However, further research is needed over weight reduction for this specific recuperator. Reaction Engines developed a heat exchanger suitable for rocket engine applications as it can withstand extremely high temperature and pressure differentials [50]. However, innovative design, high surface, and lightweight structure raise the potential for the use in micro-GT with high pressure ratio requirements. The company selected a tubular design for the SABRE (Synergetic Airbreathing and Rocket Engine) rocket engine. The heat exchanger consists of a compact array of small circular tubes containing the high-pressure fluid. The tubes follow a spiral path around a cylindrical drum in a modular arrangement for easy installation and repair. The air flows in a crossflow over the tube surfaces [51].

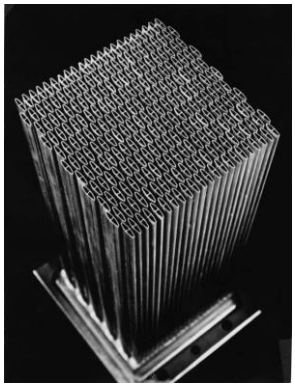

Figure 3-10: Elliptical tube recuperator [1].

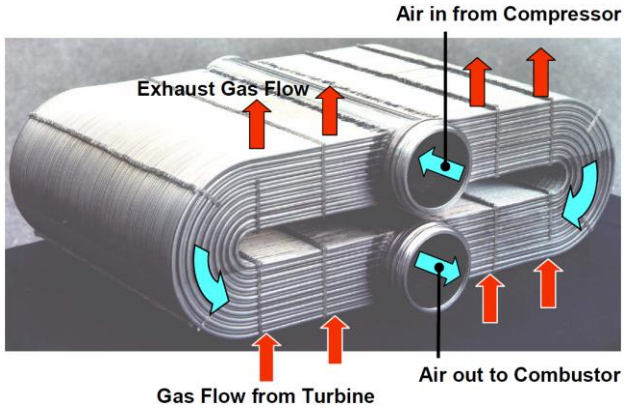

Figure 3-11: MTU profile tube heat exchanger for recuperation [52]

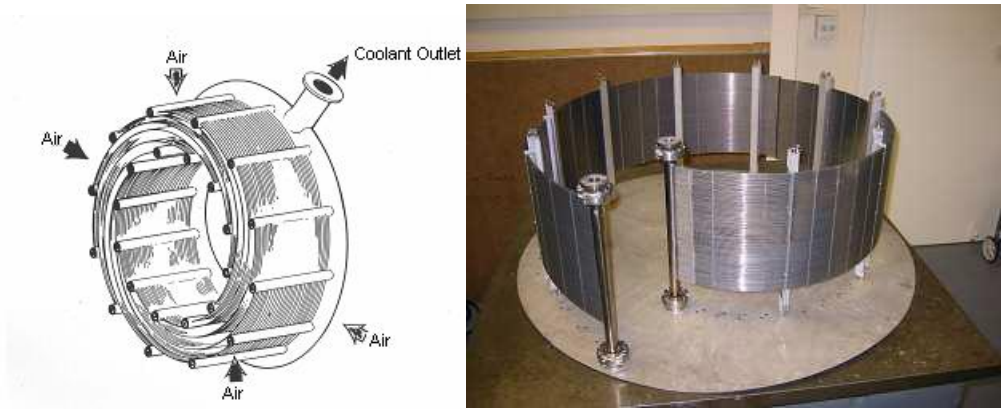

Figure 3-12: SABRE heat exchanger (a) schematic representation, (b) first prototype [50]

3.2.4 Metal Foam Heat Exchangers

The high area per unit volume makes metal foam a favourable material for light weight structures and applications that require enhanced heat transfer such as recuperators. Conventional heat exchangers can be converted into compact with incorporation of metal foams. A first category is tube and plate, the second is finned tube or tube in tube and the third is shell and tube heat exchangers, all of them filled with metal foams. The incorporation of metal foam on heat exchangers generally improved the overall performance when they were compared to hollow rectangular channels [53]. Experiments in a plate configuration used compressed Al 6101-T6 foam which decreased the thermal resistance by nearly half, compared to a current application [54]. A plate-foam heat exchanger concept (Figure 3-13), demonstrated by Kim et al using aluminium alloy [55, 56] was employed to characterise heat transfer and pressure drop of different permeabilities and porosities. A comparison with louvered fins showed similar effectiveness with metal fines and higher pressure drop [55]. Tube-in-tube configurations can be filled with metal foams inside the tube or in the annular channel [57, 58]. The analysis proved that the heat transfer performance of the foam was higher than longitudinal and spiral fins with the same surface density [56]. The effect of pore size on thermal and hydraulic properties of flat tube metal foam heat exchanger was studied [59]. In this experiment rectangular foams were brazed in between the tubes. Figure 3-14 depicts an example of flat tube metal foam heat exchanger with 10 Pores Per Inch (PPI) as pore size. A shell and tube experimental work has achieved up to 71% heat transfer enhancement [60]. The metal foam was wrapped around a metal tube. The work suggests the presence of metal foam inside the tube too, due to the inefficient heat transfer between the internal mass stream and the wall. Numerical investigation explored the performance of a metal foam baffle cut shell and tube heat exchanger (MF-BCHE), as shown in Figure 3-15 and demonstrated this as the optimum choice over given heat exchangers [61]. For common thermal efficiency and fan power, metal foam heat exchanger was smaller in size and lighter in weight than a finned one [62]. However, there was an increased manufacturing cost for the metal foam.

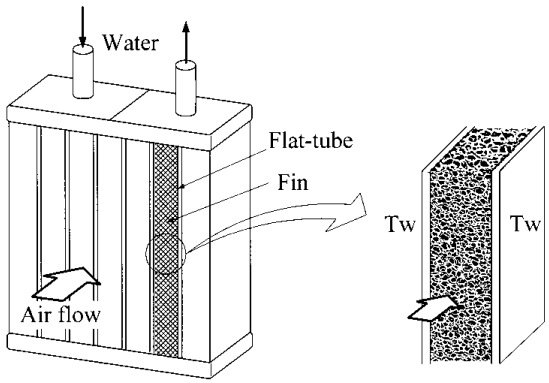

Figure 3-13: PFHE with Al alloy foam [55].

Figure 3-14: 10 PPI metal foam heat exchanger [59].

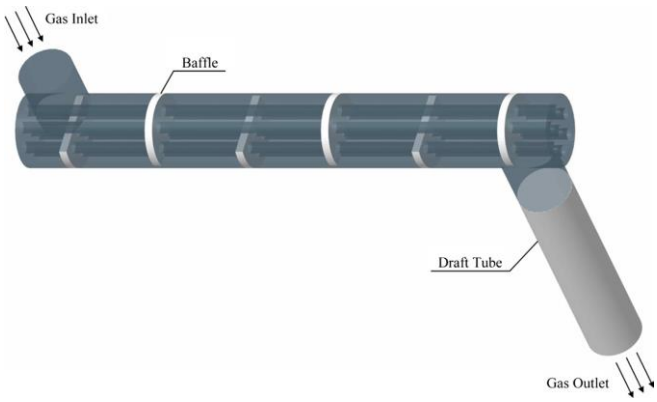

Figure 3-15: Model of metal foam baffled cut shell and tube heat exchanger (MF-BCHE) [61]

3.3 Materials and Processes

Not only should effectiveness be increased by advancements in design, but also in materials. The trend in materials and manufacturing of micro-GT components focuses on high temperature region. The most frequent existing materials used for recuperators are 347 SS and Inconel 625 depending on the cost and temperature requirements. Technological future growth of recuperators counts directly on material advancements. Operating temperature is the major limitation to material due to corrosion, oxidation, and creep deformation. The recuperator is also exposed to thermal cycling which can deteriorate in long term the sealing performance, and reliability. As a result, technology draws attention on the novel materials such as advanced alloys and ceramics, and new manufacturing methods to meet future targets for environmentally friendlier micro-GT.

The performance of high temperature materials was evaluated focusing on recuperators [23]. The use of several materials is prohibitive because of poor thermal stability. For instance, Aluminium and Copper have excellent thermal conductivity that could sharply increase the effectiveness, but their melting point falls within the range of recuperator operational temperatures. The highest temperature service of otherwise affordable 347 SS is 675 °C. The limiting factor for this stainless steel is the corrosion caused by water vapour contained in the exhaust gas. Several research activities show interest in material selection for micro-GT applications [63, 64, 65, 66]. Such materials are advanced metal alloys like stainless steel with improved oxidation resistance or creep resistance [65, 67]. Alloy 803 and Haynes 120 can extend the service temperature to 750 °C. Exposure to oxidative environment at 666 °C showed that in Haynes 120 the weight loss of Cr was only 1.5 wt.% compared to 2.2 wt% in 347 SS [23, 68]. Experimental tests proved that alloys Haynes 120, Haynes 230, and modified Alloy 803 exhibit high creep strength with former two having about twice the creep resistance of SS 347. However, Haynes 214 and Alloy 625 showed better resistance to creep rupture. Despite their eminent performance in temperatures greater than 800 °C, high material cost is restrictive for the application in micro-GT industry. Besides, high density of the metal alloys would essentially result in a lack of weight reduction.

Ceramic and Ceramic Matrix Composite (CMC) materials can be an advantageous alternative to metals due to their superior performance in terms of thermal, mechanical, and physical properties [69, 70, 71]. Apart from the turbine blades, they can also be considered as favourable materials for combustors and heat exchangers [12]. They also have low thermal expansion, high strength, and high stiffness. Additionally, their lower density compared to metal alloys, would theoretically reduce the weight of recuperator matrix by more than 50%, considering that SiC has density of 3.1 g/cm^3. However, installation and handling should be conducted with extra care, as they are known to be brittle and show poor energy absorption. SiC is recognised by the high thermal conductivity in combination with high thermal resistance and stability in corrosive media. For this reason, SiC was selected for several recuperators [4, 34, 11, 72, 73]. Aluminium Nitride (AlN) belongs to the advanced ceramics family. Numerical studies showed that the 26% higher effectiveness compared to Al2O3 is attributed to higher thermal conductivity, making this material a perfect candidate for ceramic heat exchangers [74]. A ceramic recuperator concept utilised Silicon carbon nitride (SiCN) with proved thermal stability up to 1500 °C has the potential to be stable in exhaust gas up to 1300 °C [14].

New compact designs are the result of performance requirements and necessity for novel manufacturing methods. The processes tend to be more automated aiming to reduce high labour and operational cost. The corrugation patters in PSHE are made by forming operations such as stamping or calendaring [10, 36]. LOM is an attractive method for manufacturing ceramic heat exchangers. It was used by Ceramatec, forming the shape by blending ceramic powders and organic binders and casting onto mylar film [34]. After being dried and cured, the matrix comes to the green state. At this stage micro-channels are formed, and then plates are sintered creating a monolithic structure. In addition, three process steps were investigated for ceramic recuperators manufacturing: laser cutting, laminating, and sintering by applying heat pressure and chemical solvents [75]. In printed circuit heat exchangers, channels are manufactured by chemical etching or mechanical pressing, forming very small diameters [41]. Additive manufacturing demonstrates exceptional flexibility in terms of complex shapes utilizing various materials, including metals and ceramics. Selective Laser Melting (SLM) is an additive manufacturing developing method that offers quick fabrication of custom-made heat exchangers in small sizes [76]. Currently SLM is used for development parts holding great promise for commercial heat exchangers in the future. Thus, apart from diffusion of gas state into solid phase, additive manufacturing is an option for metal or ceramic foams with periodic cellular architectures [77, 78]. Direct Laser sintering (DLS) is another technique that belongs to the category of additive manufacturing and was employed to fabricate heat exchangers [79, 80]. This method has recently gain interest showing flexibility in various materials and capabilities in unconventional designs for lightweight structures.

Bonding methods play a dominant role in heat exchanger manufacturing. In recent years welding is a preferred bonding process as it provides good sealing and straightforward manufacturing. Laser welding which promises high precision and durability in joining metal plates, has also shown capability for joining ceramic parts [81, 82]. The brazing and welding material can seriously affect the thermal conductivity due to the thermal resistance that may be introduced from the contact areas [83]. The diffusion bonding of plates in printed circuit heat exchanger allows grain growth between them [41, 84]. This kind of bonding heats the plates to near melting point temperatures while under compression, providing eliminated contact thermal resistance and high interfacial strength, comparable to that of the bulk parent material. A manufacturing method that can fall into brazing bonding category, was applied by Murray, assembling fine tubes into manifolds by electroless Nickel plating [85]. This method enabled the even distribution of nickel phosphorous braze alloy on the surfaces to be brazed. Even though extra care is taken for the performance of the core material, creep damage can also occur in the connections. Residual stresses induced by welding or brazing increase risks of leaking and failure. However, brazing is a popular method for bonding components with metal foams [15]. The wettability of the joining surface can be improved by electrodeposition process to enable compatibility with the joining component [86]. Consequently, brazing methods need more investigation for better process control and cost reduction as, in many cases, this operation is necessary. Materials and manufacturing are the major factors for the development of next generation recuperators in micro-GT industry.

3.4 Thermal and Hydraulic Performance of Advanced Materials

Low Reynolds numbers in channel flows usually have fully developed laminar flow giving a constant and low Nusselt number which is independent of Prandtl number. It has been already suggested that at low Reynolds numbers, mixing inside ducts can contribute to heat transfer enhancement, since temperature gradients can be augmented close to the wall and smoothed out away from it [87]. Components of heat transfer enhancement via mixing are tube inserts or tubes with shaped surfaces such as dimples, knurls, and corrugations [8]. An example of tube insert is coiled wire. These configurations generate a mixing effect in the flow, re-arranging the thermal energy distribution. Additionally, the temperature profile is flattened across the cross-sectional area of the tube and the temperature gradient is increased closer to the wall. This slope, and the heat transfer coefficient, approaches the equivalent turbulent profile and restores the dependence on the Prandtl number. Similar effect is promoted by porous materials [57]. Heat transfer from the foam to the fluid was found 10 times larger than heat transfer from the wall to the fluid, due to the thin boundary layer formed in the foam ligaments, as well as intense mixing in the flow [88]. This means that velocity gradient near the wall becomes steeper, making the flow field more homogenised.

Heat transfer and hydraulic performance are key characteristics for the thermohydraulic evaluation of a heat exchanger. Colburn and dimensionless friction factor may be used as metrics for the above characteristics. The Colburn factor j is adopted to describe the heat transfer expressed as a function of Nusselt and Reynolds number. The dimensionless friction factor f is an assessment for pressure drop. Both parameters significantly affect the thermal efficiency and the power output of micro-GT. The main objective for high thermohydraulic performance for the heat exchanger is j/f ratio maximisation.

Several properties are directly related to metal foam base material and porosity, but thermal conductivity is also dependent on the microstructure due to the conductive paths that are formed by the ligaments of the material. Thermal conductivity in metal foams has been investigated both experimentally and analytically in a few studies [89, 90, 91, 92, 93]. A popular experimental method for determination of effective thermal conductivity of metal foams for transient state, that can be also used for steady state, is the Laser Flash Method [94, 95, 96, 97, 98]. Most geometrical models are developed for unit cells in shapes of 2D hexagonal [99], or 3D tetrakaidecahedron with cubic nodes [100] at the intersection of ligaments. Image and geometrical analysis were performed on tetrakaidecahedron geometry with spherical nodes to determine node size and predict effective thermal conductivity [101]. No-lumps in the intersections were considered for a dodecahedron structure with 12 pentagon faces. This model did not consider heat conduction of the fluid. An analytical model Boomsma and Poulikakos [100] proved that the solid face is more dominant in terms of the overall effective conductivity, even at high porosities and high conductivity fluids. The solid phase thermal conductivity is proposed to be manipulated by the foam structure during the manufacturing process [102]. Due to the challenging determination of geometric characteristics, extensive efforts have been made to model heat transfer and flow phenomena in porous media, using such basic representations of foam microstructure [99]. Several studies have found correlations between geometric parameters. For example, parameters such as tortuosity, specific surface area, solid ligament length and diameter can be expressed as a function of porosity and mean pore diameter [103]. Most of heat transfer models are one dimensional, developed on either two- or three-dimensional cubic unit cells. Assumptions developed by existed models consider the validity of local thermal equilibrium, thermal dispersion and non Darcian effects [104]. Parametric studies show that heat transfer increases with number of pores, [105, 106] and increases with porosity until it reaches a peak at 66%, to decrease after that point [107]. A comparison with plain tubes showed that the heat transfer performance of metal foam filled tubes had up to 40 times higher heat transfer performance [57].

The flow of a fluid through a porous medium follows Darcy's law, considering the linear relationship between pressure drop and velocity as well as the viscous force in the material. Extended versions of the law include the Forchheimer equation, which considers the inertial effect of velocity, or add the Brickman term. At constant velocity, the pressure drop is affected by the porous media microstructure [102]. Permeability K is an important parameter for pressure drop that was managed to be expressed

empirically as function of porosity and ligament diameter [99]. Correlations were also found for inertial coefficient as function of foam main geometrical features [90, 103]. Pore density and porosity give the opposite effect on pressure drop, in comparison to heat transfer. As a result, optimal porosity was found to range between 0.85 and 0.95%, considering both heat transfer and pressure drop [102]. Similar findings from a study in a parallel-plate channel with metal foams suggest an optimal performance, which is evaluated at maximised $j/f^{1/3}$, at the same porosity range and pore density between 10 PPI and 20 PPI [108]. These geometric features should be taken into consideration to create a lightweight and compact heat exchanger.

3.5 Summary

The current study presented a summary of late designs of compact recuperators considering the types of recuperators, their performance in micro-GT, materials and processes, and thermohydraulic performance of porous media as a compact solution for the heat management in micro-GT. Innovation in compact heat exchanger technology is stepping forward focusing on novel and more compact design as well as materials selection for a cost-effective micro-GT. The goal for heat management is to include a recuperator in the system, combining high effectiveness and low pressure drop.

Technological development in manufacturing has achieved more compact designs in comparison to conventional heat exchangers, with stronger bonds in the connections, contributing to better mechanical integrity. Apart from high compactness, recent advancements in additive manufacturing can achieve more complex shapes and flexibility in material utilisation. The most important parameter in materials selection is the TIT, which is the limiting factor for the thermal efficiency. Low-cost materials are characterised by high performance in low temperatures, losing these advantages at increased temperatures. Currently, economical primary surface metal recuperators achieve efficiency up to 35%. Although super alloys can achieve thermal and mechanical requirements, they lead to high material cost. Therefore, ceramic materials are an appropriate solution in materials selection processes since they combine low density, high thermal conductivity, resistance to creep, and resistance to corrosion even at elevated temperatures. It is expected that ceramic recuperators will increase the thermal efficiency at approximately 40%. Further effort is needed to reduce cost in materials and manufacturing to produce an affordable lightweight recuperator.

Heat exchangers embedded with porous media such as metal foams are reviewed. The heat transfer performance and pressure drop were examined at a macroscopic scale. Porous structures have substantial advantages in heat exchangers applications over commercially available heat exchangers. They increase the area over volume of the heat exchanger and enhance flow mixing. This combination is beneficial for the component, since effectiveness is amplified by increased convective heat transfer due flow mixing and high compactness. The microstructure features of porous media are used to find heat transfer correlations. Despite enhanced heat transfer rate, reduction of permeability and porosity causes pressure drop rise. There is a trade-off between heat transfer rate and pressure drop for a specific application. Usage of ceramic materials, in combination with recent manufacturing methods, and a novel compact design, can produce in the future recuperators that offer to micro-GT a comparable efficiency to internal combustion engines.

4. Definition of Methods of Analysis of Heat Transfer Performance of Metallic Foams

4.1 Definition of Methods of Analysis of Heat Transfer and Pressure Drop Performance of Porous Media Filled Recuperators for Micro-GT Applications

This report is part of the milestone 10 entitled “Definition of methods of analysis of heat transfer and pressure drop performance of porous media filled recuperators for micro-GT applications”. The aim is to develop an innovative heat exchanger with advanced materials for micro-GT applications for high

efficiency, low pressure drop, and low weight. The methodology for performance is divided in two tasks namely, steady state one dimensional modelling, and experimental analysis with CFD validation.

4.2 Steady-State One-Dimensional Modelling

In this section, thermal-hydraulic performance of a heat exchanger filled with porous media, is discussed. The heat exchanger is considered as a recuperator working in a Brayton cycle. The recuperator is a double pipe heat exchanger in counterflow arrangement filled with open cell metal foam on hot and cold side. The component uses the thermal energy of micro-GT gases to heat compressed air before it enters the combustion chamber. The goal is to evaluate the impact of the recuperator geometry features on the thermal efficiency, power output and weight savings in a micro gas turbine. Models for global heat transfer coefficient, effective thermal conductivity, surface area and pressure drop of porous media filled heat exchanger are adopted and implemented in python code.
The most common methods for the thermal design of heat exchangers are the Logarithmic Mean Temperature Difference (LMTD) and the effectiveness - Number of Transfer Units (ε-NTU) method. The second method needs to specify two inlet temperatures. The corresponding value of UA can be calculated, and outlet temperatures can be determined from the equations of the corresponding flow arrangement. These methods are suitable for recuperators as they assume that the heat transfer fluids have constant specific heat capacity. In this study the ε-NTU method is adopted. It is assumed that the heat transfer occurs in one dimension. Fouling and contact thermal resistances are neglected. Additional simplifying assumptions consider that heat losses and kinetic and potential energies are ignored. These assumptions comprise common approaches for heat exchanger study, to calculate effectiveness and outlet temperatures.

4.3 Overall Heat Transfer Coefficient of Recuperator Filled with Porous Media

Based on the above assumptions, the heat transfer between compressed air and hot gases is calculated according to the following equations:

$$\dot{Q} = U \cdot A_{exc} \cdot LMTD = \dot{m}_{gas} \cdot Cp_{gas} \cdot \left(T_{h,in} - T_{h,out}\right) = \dot{m}_{air} \cdot Cp_{air} \cdot \left(T_{h,out} - T_{h,in}\right) \quad (1)$$

Parallel flow and counter flow are common symmetrical flow arrangements. Counterflow achieves higher values of effectiveness. The LMTD is calculated as a function of inlet and outlet temperatures for both streams as defined by Eq. 2 for the counterflow arrangement:

$$LMTD = \frac{\left(T_{h,in} - T_{c,out}\right) - \left(T_{h,out} - T_{c,in}\right)}{ln\left[\frac{\left(T_{h,in} - T_{c,out}\right)}{\left(T_{h,out} - T_{c,in}\right)}\right]} \quad (2)$$

The overall heat transfer coefficient can be calculated using heat transfer resistance according to Eq. 3.

$$R_{tot} = \frac{1}{UA_{exc}} = \frac{1}{A_{gas} \cdot h_{gas}} + \frac{\left[ln\left(\frac{r_o}{r_i}\right)\right]}{2\pi L \cdot k_{wall}} + \frac{1}{A_{air} \cdot h_{air}} \quad (3)$$

All thermophysical properties are taken at the mean temperature. A value of exit temperatures is assumed for each stream, and an iterative process is followed until there is convergence.

4.4 Performance Modelling of Recuperator Filled with Porous Media

Examples of various models describing the thermohydraulic performance are gleaned inTable 4-1. These models result from analytical, experimental, or numerical analysis. The models that describe the thermal performance of porous media combined to define the overall heat transfer coefficient.

Table 4-1 Examples of models of thermohydraulic performance of porous media

Models	Examples
Geometry	Calmidi and Mahajan [1]
Effective thermal conductivity	Boomsma and Poulikakos [2], Calmidi and Mahajan [3], Nawaz [4]
Heat transfer	Zukauskas [5], Mancin et al [6], Mancin et al [7]
Fin effects	Mancin et al [6], Mancin et al [7], Nawaz [4]
Pressure-drop	Calmidi and Mahajan [1]

The model was verified using CFD results of Chen et al [8] and comparing the temperature distribution along the axis parallel to the flow in the heat exchanger between CFD and 1 dimensional analysis. The outputs of exit temperatures and recuperator effectiveness are less sensitive by applying different models of heat transfer and thermal conductivity than the fin effect models. The model that produces the smallest error was selected to carry out the optimisation process. The multi-objective optimisation sets 3 objective functions. At component level the three objectives effectiveness maximization, and pressure drop and weight minimization. At system level the model maximises the thermal efficiency and power output and minimises heat exchanger weight. The optimum set of solutions are selected to form the pareto front.

4.5 Experimental Methods

The main initiative is the experimental study of thermohydraulic performance of porous media. The experimental set up has considered the requirements for waste heat recovery and heat management in micro-Gas Turbine systems. Initially the experimental set up has been designed and assembled. Copper metal foams were provided from Laboratory of Physical Metallurgy of AUTH. The set-up consists of hot and cold-water circuits. This achieves a quick temperature change of water. The sample was assembled with a press fit inside a copper tube which was placed perpendicularly in a plexiglass pipe. Cold air was flowing constantly inside the plexiglass to cool the test section. Liquid Thermochromic Crystals (TLC) were provided in adhesive films and were placed on the surface of copper tube at the copper foam location, to allow the visualization of temperature change. When the hot water reaches a steady state, a change by a three-way valve stops the hot water and allows the cold-water flow. The TLC colour change on the surface of the copper tube is recorded during the whole procedure by a camera. The video was inserted into an algorithm which converts the colour from TLC into temperature using Matlab Simulink. An example of temperature distribution is shown in the figure below. The experimental data were used in a considering one dimensional heat transfer in a semi-finite body with convection boundary conditions The cooling effectiveness, and heat transfer coefficient were calculated during these experiments including Nusselt and Reynolds numbers. The plan includes more experiments in the next steps with TLC and pressure drop measurements to establish the performance of foams with different geometrical characteristics.

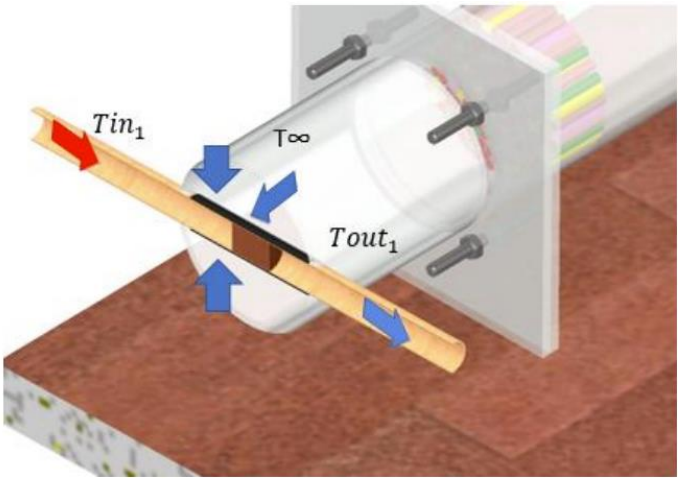

Experimental set-up. Test section.

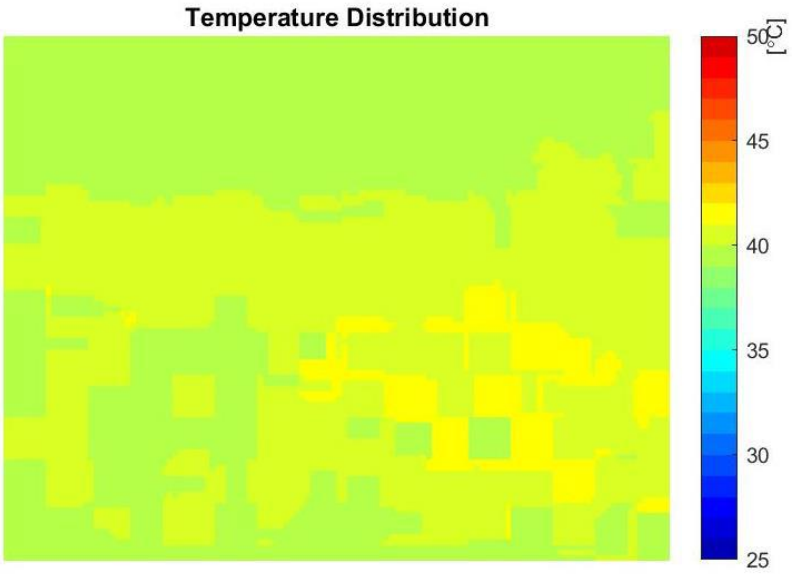

Wall temperature distribution on the TLC surface after video processing in Simulink.

4.6 Experimental Validation with CFD

A CFD model is also needed for the next steps for validation with the experimental results. There are various approaches to construct 3D geometry of porous materials including computed tomography, metallographic serial sectioning, and volume tessellation techniques. One of those techniques will be selected for the numerical analysis depending on the error that they produce on the porosity, and specific area density. After the construction of the model, the numerical analysis will be performed using a commercial software and the governing equations will be solved.

References

[1] C. F. McDonald, "Recuperator considerations for future higher efficiency microturbines," *Applied Thermal Engineering,* vol. 23, pp. 1463-1487, 2003.

[2] R. K. Shah, "Compact Heat Exchangers for Microturbines," in *Fifth International Conference on Enchanced, Compact and Ultra-Compact Heat Exchangers: Science, Engineering and Technology*, Hoboken, 2005.

[3] C. F. McDonald, "Low Cost Recuperator Concept for Microturbine Applications," in *ASME Turbo Expo 2000,* Munich, 2000.

[4] C. F. McDonald and D. G. Wilson, "The utilization of recuperated and regenerated engine cycles for high-efficiency gas turbines in the 21st century," *Applied Thermal Engineering,* vol. 16, no. 8-9, pp. 635-653, 1996.

[5] B. Tsai and Y. L. Wang, "A novel Swiss-Roll recuperator for the microturbine engine," *Applied Thermal Engineering,* vol. 29, pp. 216-223, 2009.

[6] C. Zhang, M. Kerler and V. Gümmer, "Evaluation of the Fuel Saving Potential Regarding Recuperated Helicopter Flight Conditions," in *ASME*, Oslo, 2018.

[7] V. Gesellschaft, VDI Heat Atlas, Springer, 2010.

[8] J. E. Hesselgreaves, R. Law and D. Reay, Compact Heat Exchangers: Selection, Design and Operation, Butterworth-Heinemann, 2016.

[9] A. F. Massardo, C. F. McDonald and T. Korakianitis, "Microturbine/Fuel-Cell Coupling for High-Efficiency Electrical-Power Generation," *Journal of Engineering for Gas Turbines and Power,* vol. 124, no. 1, pp. 110-116, 2002.

[10] C. F. McDonald, "Low-cost compact primary surface recuperator concept for microturbines," *Applied Thermal Engineering,* vol. 20, no. 5, pp. 471-497, 2000.

[11] K. Parker and M. Coombs, "Development in plate-fin heat exchangers," *ASME Publication HTD,* vol. 10, p. 171–179, 1979.

[12] C. F. McDonald and C. Rogers, "Small recuperated ceramic microturbine demonstrator concept.," *Applied Thermal Engineering,* vol. 28, pp. 60-74, 2008.

[13] N. Michailidis, F. Stergioudi, A. Tsouknidas and E. Pavlidou, "Compressive response of Al-foams produced via a powder sintering process based on a leachable space-holder material," *Materials Science and Engineering: A,* vol. 528, no. 3, pp. 1662-1667, 2011.

[14] B. G. Carman, J. S. Kapat, L. C. Chow and L. An, "Impact of a Ceramic Microchannel Heat Exchanger on a Micro Turbine," in *ASME,* Amsterdam, 2002.

[15] X. Han, Q. Wang, Y. Park, C. T'Joen, A. Sommers and A. Jacobi, "A Review of Metal Foam and Metal Matrix Composites for Heat Exchangers and Heat Sinks," *Heat Transfer Engineering,* vol. 33, no. 12, pp. 991-1009, 2012.

[16] P. S. Liu and K. M. Liang, "Functional Materials of Porous Metals Made by P/M, Electroplating and Some Other Techniques," *Journal of Materials Science,* vol. 36, pp. 5059-5072, 2001.

[17] H. Tang, J. Liao and J. Zhu, "Porous Metals of Northwest Institute for Non-ferrous Metal Research," *Materials Science Forum,* Vols. 534-536, pp. 1281-1284, 2007.

[18] L. Tuchinskiy, "Novel Fabrication Technology for Metal Foam," *Journal of Advanced Materials,* vol. 37, pp. 60-65, 2005.

[19] J. Banhart, J. Baumeister, and M. Weber, "Metal Foams Near Commercialization," *Metal Powder Report,* vol. 52, pp. 38-41, 1997.

[20] F. Djamaluddin, S. Abdullah, A. K. Ariffin and Z. M. Nopiah, "Multi objective optimization of foam-filled circular tubes for quasi-static and dynamic responses," *Latin American Journal of Solids and Structures,* vol. 12, no. 6, pp. 1126-1143, 2015.

[21] Z. Wang, J. Shen, G. Lu and L. Zhao, "Compressive behavior of closed-cell aluminum alloy foams at medium strain rates," *Materials Science and Engineering: A,* vol. 528, no. 6, pp. 2326-2330, 2011.

[22] N. Michailidis, F. Stergioudi and A. Tsouknidas, "Deformation and energy absorption properties of powder-metallurgy produced Al foams," *Materials Science and Engineering: A,* vol. 528, no. 24, pp. 7222-7227, 2011.

[23] A. Aquaro and D. Pieve, “High temperature heat exchangers for power plants: Performance of advanced metallic recuperators,” *Applied Thermal Engineering,* vol. 27, no. 2-3, pp. 389-400, 2007.

[24] C. Zhang, M. Kerler and V. Volker Gümmer, “Evaluation of the fuel saving potential regarding recuperated helicopter flight conditions,” in *ASME,* Oslo, 2018.

[25] C. F. McDonald and C. Rodgers, “Heat-exchanged propulsion gas turbines: a candidate for future lower SFC and reduced-emmision military and civil aeroengines,” in *ASME,* Orlando, 2009.

[26] “Proe 90TM recuperator for microturbine applications,” in *ASME Turbo Expo 2002,* Amsterdam, 2002.

[27] M. E. Ward and M. D. Stephenson, “Primary surface recuperator durability and applications,” San Diego, 1995.

[28] E. Utriainen and B. Sundén, “Recuperators in Gas Turbine Systems,” in *ASME 1998 International Gas Turbine and Aeroengine Congress and Exhibition,* Stockholm, 1998.

[29] C. F. McDonald, A. F. Massardo, C. Rogers and A. Stone, “Recuperated gas turbine aeroengines, part II: engine design studies following early development testing,” *Aircraft Engineering and Aerospace Technology: An International Journal,* vol. 80, no. 3, pp. 280-294, 2008.

[30] A. Muley and B. Sundén, “Advances in recuperator technology for gas turbine systems,” in *ASME 2003 International Mechanical Engineering Congress and Exposition,* Washington, 2003.

[31] G. Xiao, T. Yang, H. Liu, N. Dong, M. Ferrari, M. Li, Z. Luo, K. Cen and M. Ni, “Recuperators for micro gas turbines: A review,” *Applied Energy,* vol. 197, pp. 83-99, 2017.

[32] G. Lagerström and M. Xie, “High Performance and Cost Effective Recuperator for Micro-Gas Turbines,” in *ASME,* Amsterdam, 2002.

[33] J. Kesseli, T. Wolf, J. Nash and S. Freedman, “Micro, industrial, and Advanced Gas Turbines Employing Recuperators,” in *ASME,* Atlanta, 2003.

[34] M. A. Wilson, K. Recknagle and K. Brooks, “Design and development of a low-cost, high temperature Silicon Carbide micro-channel recuperator,” in *ASME,* Reno, 2005.

[35] B. Treece and R. McKeirnan, “Microturbine Recuperator Manufacturing and Operating Experience,” in *ASME,* Amsterdam, 2002.

[36] H. Antoine and L. Prieels, “The ACTE spiral recuperator for gas turbine engines,” in *ASME,* Amsterdam, 2002.

[37] S. G. Kim, Y. Lee, Y. Ahn and J. I. Lee, “CFD aided approach to design printed circuit heat exchangers for supercritical CO2 Brayton,” *Annuals of Nuclear,* vol. 92, pp. 175-185, 2016.

[38] A. A. Gkountas, L. T. Benos, K. S. Nikas and I. Sarris, “Heat transfer improvement by an Al2O3-water nanofluid coolant in printed-circuit heat exchangers for supercritical CO2 Brayton cycle,” *Thermal science and engineering progress,* vol. 20, 2020.

[39] “Heatric,” [Online]. Available: https://www.heatric.com/index.html.

[40] D. E. Kim, M. H. Kim, J. E. Cha and S. O. Kim, “Numerical investigation on thermal–hydraulic performance of new printed circuit heat exchanger model,” *Nuclear Engineering and Design,* vol. 238, no. 12, pp. 3269-3276, 2008.

[41] R. Le Pierres, D. Southall and S. Osborne, “Impact of Mechanical Design Issues on Printed Circuit Heat Exchangers,” in *Supercritical CO2 Power Cycle Symposium,* Boulder, 2011.

[42] X. Xu, T. Ma, L. Li, M. Zeng, Y. Chen, Y. Huang and Q. Wang, “Optimization of fin arrangement and channel configuration in an airfoil fin PCHE for supercritical CO2 cycle,” *Applied Thermal Engineering,* vol. 70, no. 1, pp. 867-875, 2014.

[43] T. L. Ngo, Y. Kato, K. Nikitin and T. Ishizuka, “Heat transfer and pressure drop correlations of microchannel heat exchangers with S-shaped and zigzag fins for carbon dioxide cycles,” *Experimental Thermal and Fluid Science,* vol. 32, no. 2, pp. 560-570, 2007.

[44] k. Takase, H. Furukawa and K. Nakano, “A preliminary study of of an Inter-Cooled and Recuperative Microgasturbine Below 300 kW,” in *ASME,* Amsterdam, 2002.

[45] J. I. Oswald, D. A. Dawson and L. A. Clawley, “A new durable gas turbine recuperator,” in *Int Gas Turbine Aeroengine Congress,* Indianapolis, 1999.

[46] F. D. Doty, G. Hosford, J. B. Spitzmesser and J. D. Jones, “The Microtube Strip Heat Exchanger,” *Heat Transfer Engineering,* vol. 12, no. 3, pp. 31-41, 1991.

[47] G. Wilfert, J. Sieber, A. Rolt, A. Touyeras and N. Baker, “New environmental friendly aero engine core concepts,” in *ISABE,* Beijing, 2007.

[48] H. Schonenborn, E. Ebert, B. Simon and P. Storm, “Thermomechanical Design of a Heat Exchanger for a Recuperative Aero Engine,” in *ASME,* Vienna, 2004.

[49] C. Albanakis, K. Yakinthos, K. Kritikos, D. Missirlis, A. Goulas and P. Storm, “The effect of heat transfer on the pressure drop through a heat exchanger for aero engine applications,” *Applied Thermal Engineering,* vol. 29, no. 4, pp. 634-644, 2009.

[50] H. Webber, S. Feast and A. Bond, “Heat exchanger design in combined cycle engines,” *Journal of the British Interplanetary Society,* vol. 62, pp. 122-130, 2009.

[51] R. Varvill, “Heat exchanger development at Reaction Engines Ltd.,” *Acta Astronautica,* vol. 66, p. 1468–1474, 2010.

[52] S. Boggia and K. Rüd., “Intercooled Recuperated Gas Turbine Engine Concept,” in *41st AIAA/ASME/SAE/ASEE Joint Propulsion Conference & Exhibit,* Tucson, 2005.

[53] P. Hafeez, L. Esmaeelpanah, S. Chandra and J. Mostaghimi, “Heat Transfer Through Metal-Foam Heat Exchanger at Higher Temperature,” in *ASME,* Minneapolis, 2013.

[54] K. Boomsma and D. Poulikakos, “Metal foams as compact high performance heat exchangers,” *Mechanics of Materials,* vol. 35, no. 12, pp. 1161-1176, 2003.

[55] S. Y. Kim, J. W. Paek and B. H. Kang, “Flow and heat transfer correlations for porous fin in a plate-fin heat exchanger,” *Journal of Heat Transfer,* vol. 122, pp. 572-578, 2000.

[56] S. Y. Kim, B. H. Kang and J. Kim, “Forced convection from aluminum foam materials in an asymmetrically heated channel,” *International Journal of Heat and Mass Transfer,* vol. 44, pp. 1451-1454, 2001.

[57] W. Lu, C. Y. Zhao and S. A. Tassou, “Thermal analysis on metal-foam filled heat exchangers. Part I: Metal-foam filled pipes,” *International journal of heat and mass transfer,* vol. 49, no. 15-16, pp. 2751-2761, 2006.

[58] C. Y. Zhao, W. Lu and S. A. Tassou, “Thermal analysis on metal-foam filled heat exchangers. Part II: Tube heat exchangers,” *International Journal of Heat and Mass Transfer,* vol. 49, no. 15-16, pp. 2762-2770, 2006.

[59] K. Nawaz, J. Bock and A. M. Jacobi, “Thermal-hydraulic performance of metal foam heat exchangers under dry operating conditions,” *Applied Thermal Engineering,* vol. 119, pp. 222-232, 2017.

[60] T. Fiedler , R. Moore and N. Movahedi, “Manufacturing and Characterization of Tube-Filled ZA27 Metal Foam Heat Exchangers,” *Metals,* vol. 11, no. 8, 2021.

[61] T. Chen, G. Shu, H. Tian, T. Zhao, H. Zhang and Z. Zhang, “Performance evaluation of metal-foam baffle exhaust heat exchanger for waste heat recovery,” *Applied Energy,* vol. 266, 2020.

[62] Z. Dai, K. Nawaz, Y. Park, Q. Chen and A. Jacobi, “A comparison of metal-foam heat exchangers to compact multilouver designs for air-side heat transfer applications,” *Heat transfer engineering,* vol. 33, no. 1, pp. 21-30, 2012.

[63] B. A. Pint, K. L. More, R. Trejo and E. Lara-Curzio, “Comparison of recuperator alloy degradation in laboratory and engine testing,” in *ASME,* Barcelona, 2006.

[64] E. Lara-Curzio, R. Trejo, K. L. More, P. A. Maziasz and B. A. Pint, “Screening and evaluation of metallic materials for microturbine recuperators,” in *ASME,* Vienna, 2004.

[65] M. A. Harper, G. D. Smith, P. J. Maziasz and R. W. Swindeman, “Materials selection for high temperature metal recuperators,” in *ASME,* New Orleans, 2001.

[66] B. A. Pint, “Stainless steels with improved oxidation resistance for recuperators,” *Journal of Engineering of Gas Turbines and Power,* vol. 128, no. 2, pp. 370-376, 2006.

[67] P. J. Maziasz and R. W. Swindeman, “Selecting and developing advanced alloys for creep resistance for microturbine recuperator applications,” in *ASME,* New Orleans, 2001.

[68] W. L. Matthews, K. L. More and L. R. Walker, “Long-term microturbine exposure of an advanced alloy for microturbine primary surface recuperators,” in *ASME,* Berlin, 2008.

[69] F. S. Moghanlou, M. Vajdi, A. Motallebzadeh, J. Sha, M. Shokouhimehr and M. M. Asl, “Numerical analyses of heat transfer and thermal stress in a ZrB2 gas turbine stator blade,” *Ceramics International,* vol. 45, no. 14, pp. 17742-17750, 2019.

[70] J. B. Wachtman, W. R. Cannon and M. J. Matthewson, Mechanical Properties of Ceramics, Wiley, 2009.

[71] J. Silvestre, N. Silvestre and J. de Brito, “An overview on the improvement of mechanical properties of ceramics nanocomposites,” *Journal of Nanomaterials,* vol. 2015, 2015.

[72] T. Fend, W. Völker, R. Miebach, O. Smirnova, D. Gonsior, D. Schöllgen and P. Rietbrock, "Experimental investigation of compact silicon carbide heat exchangers for high temperatures," *International Journal of Heat and Mass Transfer,* vol. 54, no. 19-20, pp. 4175-4181, 2011.

[73] R. J. Kee, B. B. Almand, J. Blasi, B. L. Rosen, M. Hartmann, N. P. Sullivan, H. Zhu, A. R. Manerbino, S. Menzer, W. G. Coors and J. L. Martin, "The design, fabrication, and evaluation of a ceramic counter-flow microchannel heat exchanger," *Applied Thermal Engineering,* vol. 31, no. 11-12, pp. 2004-2012, 2011.

[74] M. Fattahi, K. Vaferi, M. Vajdi, F. S. Moghanlou, A. S. Namini and M. S. Asl, "Aluminum nitride as an alternative ceramic for fabrication of microchannel heat exchangers: A numerical study," *Ceramics International,* vol. 46, no. 8, pp. 11647-11657, 2020.

[75] M. M. Kelly, M.-J. Pan, S. Atre, G. Rancourt, A. Heyes and M. J. Vick, "Ceramic Micro Channel Recuperator Fabrication Methods for Small Gas Turbine Engines," in *ASME,* Copenhagen, 2012.

[76] S. Tsopanos, C. J. Sutcliffe and I. Owen, "The Manufacture of Micro Cross-Flow Heat Exchangers by Selective Laser Melting," in *Enhanced, Compact and Ultra-Compact Heat Exchangers,* Whistler, 2005.

[77] G. Bianchi, S. Gianella and A. Ortona, "Design and additive manufacturing of periodic ceramic architectures," *Journal of Ceramic Science and Technology,* 2017.

[78] J. Y. Ho, K. C. Leong and T. N. Wong, "Additively-manufactured metallic porous lattice heat exchangers for air-side heat transfer enhancement," *International Journal of Heat and Mass Transfer,* vol. 150, 2020.

[79] M. A. Arie, A. H. Shooshtari, V. V. Rao, S. V. Dessiatoun and M. M. Ohadi, "Air-Side Heat Transfer Enhancement Utilizing Design Optimization and an Additive Manufacturing Technique," *Journal of Heat Transfer,* vol. 139, no. 3, 2017.

[80] X. Zhang, R. Tiwari, A. H. Shoushtari and M. M. Ohadi, "An additively manufactured metallic manifold-microchannel heat exchanger for high temperature applications," *Applied Thermal Engineering,* vol. 143, pp. 899-908, 2018.

[81] M. Rohde, I. Südmeyer, A. Urbanek and M. Torgue, "Joining of Alumina and Steel by A Laser Supported Brazing Process," *Ceramics International,* vol. 35, pp. 333-337, 2009.

[82] W. Lippmann, J. Knorr, R. Wolf, R. Rasper, H. Exner, A. M. Reinecke, M. Nieher and R. Schreiber, "Laser Joining of Silicon Carbide - A New Technology for Ultra - High Temperature Resistant Joints," *Nuclear Engineering and Design,* vol. 321, pp. 151-161, 2004.

[83] T. Boger and A. K. Heibel, "Heat transfer in conductive monolith structures," *Chemical Engineering Science,* vol. 60, no. 7, pp. 1823-1835, 2005.

[84] D. Southall, "Diffusion Bonding in Compact Heat Exchangers," in *SCO2 Power Cycle Symposium 2011,* Tokyo, 2009.

[85] J. J. Murray, C. M. Hempsell and A. Bond, "An experimental precooler for airbreathing rocket engines," *JBIS,* vol. 54, pp. 199-209, 2001.

[86] S. Guarino, M. Barbieri, P. Pasqualino and G. Bella, “Fabrication and Characterization of an Innovative Heat Exchanger with Open Cell Aluminum Foams,” *Energy Procedia,* vol. 118, pp. 227-232, 2017.

[87] R. L. Webb, Principles of Enhanced Heat Transfer, New York: John Wiley & Sons, 1994.

[88] F. H. Li and T. H. Van der Meer, “Heat Transfer Enhancement by Metallic Foams,” in *13th International Heat Transfer Conference*, Sydney, 2006.

[89] A. Bhattacharya, V. V. Calmidi and R. L. Mahajan, “Thermophysical properties of high porosity metal foams,” *Internaltional Journal of Heat and Mass Transfer,* vol. 45, pp. 1017-1031, 2002.

[90] V. V. Calmidi and R. L. Mahajan, “The effective thermal conductivity of high porosity fibrous metal foams,” *ASME Journal of Heat Transfer,* vol. 212, pp. 466-471, 1999.

[91] J. W. Pack, B. H. Kang, S. Y. Kim and J. M. Hyun, “Effective thermal conductivity and permeability of aluminum foam materials,” *Internaltional Journal of Thermophysics,* vol. 21, no. 2, pp. 453-464, 2000.

[92] C. Y. Zhao, T. J. Lu, H. P. Hodson and J. D. Jackson, “The temperature dependence of effective thermal conductivity of open-celled steel alloy foams,” *Materials Science and Engineering: A,* vol. 367, p. 123–131, 2004.

[93] R. Singh and H. S. Kasana, “Computational aspects of effective thermal conductivity of highly porous metal foams,” *Applied Thermal Engineering,* vol. 24, no. 13, pp. 1841-1849, 2004.

[94] R. Wulf, M. A. Mendes, V. Skibina, A. Al-Zoubi, D. Trimis, S. Ray and U. Gross, “Experimental and numerical determination of effective thermal conductivity of open cell FeCrAl-alloy metal foams,” *International Journal of Thermal Sciences,* vol. 86, pp. 95-103, 2014.

[95] K. Lafdi, M. Almajali and O. Huzayyin, “Thermal properties of copper-coated carbon foams,” *Carbon,* vol. 47, pp. 2620-2626, 2009.

[96] J. Sauerhering, O. Reutter, T. Fend, S. Angel and R. Pitz-Paal, “Temperature Dependency of the Effective Thermal Conductivity of Nickel Based Metal Foams,” in *ASME*, Limerick, 2006.

[97] W. Hohenauer and D. Lager, “Flash Methods to Examine Diffusivity and Thermal Conductivity of Metal Foams: A Comparison with Data of a Comparative Set-Up,” in *30 ITCC 17 ITES*, Pittsburgh, 2009.

[98] “Digital Twin of a Laser Flash Experiment Helps to Assess the Thermal Performance of Metal Foams,” *hal-03528820,* 2022.

[99] V. V. Calmidi and R. L. Mahajan, “Forced Convection in High Porosity Metal Foams,” *Journal of Heat Transfer,* vol. 122, p. 557–565, 2000.

[100] K. Boomsma and D. Poulikakos, “On the Effective Thermal Conductivity of a Three Dimensionally Structured Fluid Saturated Metal Foam,” *International Journal of Heat and Mass Transfer,* vol. 44, p. 827–836, 2001.

[101] E. N. Schmierer and A. Razani, “Self-consistent open-celled metal foam model for thermal applications,” *Journal of Heat Transfer,* vol. 128, no. 11, pp. 1194-1203, 2006.

[102] C. Y. Zhao, T. Kim, T. J. Lu and H. P. Hodson, “Thermal Transport in High Porosity Cellular Metal Foams,” *Journal of Thermophysics and Heat Transfer,* vol. 18, no. 3, 2004.

[103] P. Du Plessis, A. Montillet, J. Comiti and J. Legrand, “Pressure drop prediction for flow through high porosity metallic foams,” *Chemical Engineering Schience,* vol. 49, no. 21, p. 3545–3553, 1994.

[104] A. Amiri, K. Vafai and T. M. Kuzay, “Effects Of Boundary Conditions On Non-Darcian Heat Transfer Through Porous Media And Experimental Comparisons,” *Numerical Heat Transfer Part A: Applications,* vol. 27, no. 6, pp. 651-664, 1995.

[105] D. P. Haack, K. R. Butcher, T. Kim and T. J. Lu, “Novel lightweight metal foam heat exchangers,” in *ASME,* New York, 2001.

[106] G. Trilok and N. Gnanasekaran, “Numerical study on maximizing heat transfer and minimizing flow resistance behavior of metal foams owing to their structural properties,” *International Journal of Thermal Sciences,* vol. 159, 159.

[107] L. Zhang, D. Mullen, K. Lynn and Y. Zhao, “Heat transfer performance of copper foam fabricated by lost carbonate sintering process,” *MRS Online Proceedings Library (OPL),* vol. 1188, p. 83–88, 2009.

[108] H. J. Xu, Z. G. Qu and W. Q. Tao, “Thermal transport analysis in parallel-plate channel filled with open-celled metallic foams,” *International Communications in Heat and Mass Transfer,* vol. 38, p. 868–873, 2011.

[109] E. Utriainen and B. Sundén, “A comparison of some heat transfer surfaces for small gas turbine recuperators,” in *ASME Turbo Expo 2001*, New Orleans, 2001.

[110] W. Qiuwang, L. Hongxia, X. Gongnan, Z. Min, L. Laiqin and F. ZhenPing, “Genetic Algorithm Optimization for Primary Surfaces Recuperator of Microturbine,” *Journal of Engineering for Gas Turbines and Power,* vol. 129, no. 2, pp. 436-442, 2007.

[111] S. R. Howard and P. S. Korinko, “Vacuum Furnace Brazing Open Cell Reticulated Foam to Stainless Steel Tubing,” in *International Brazing and Soldering Conference,*, San Diego, 2003.

[112] W. J. Matthews, K. L. More and L. R. Walker, “Comparison of three microturbine primary surface recuperator alloys,” *Journal of Engineering for Gas Turbines and Power,* vol. 132, no. 2, 2010.

[113] V. V. Calmidi and R. L. Mahajan, “Forced Convection in High Porosity Metal Foams,” Journal of Heat Transfer, vol. 122, p. 557–565, 2000.

[114] K. Boomsma and D. Poulikakos, “On the Effective Thermal Conductivity of a Three Dimensionally Structured Fluid Saturated Metal Foam,” International Journal of Heat and Mass Transfer, vol. 44, p. 827–836, 2001.

[115] V. V. Calmidi and R. L. Mahajan, “The effective thermal conductivity of high porosity fibrous metal foams,” ASME Journal of Heat Transfer, vol. 212, pp. 466-471, 1999.

[116] K. Nawaz, J. Bock and A. M. Jacobi, “Thermal-hydraulic performance of metal foam heat exchangers under dry operating conditions,” Applied Thermal Engineering, vol. 119, pp. 222-232, 2017.

[117] A. Zukauskas, “Heat Transfer from Tubes in Crossfow,” Advances in Heat Transfer, vol. 8, pp. 93-160, 1972.

[118] S. Mancin, C. Zilio, A. Cavallini and L. Rossetto, “Heat transfer during air flow in aluminium foams,” International Journal of Heat and Mass Transfer, vol. 53, p. 4976–4984, 2010.

[119] S. Mancin, C. Zilio, A. Diani and L. Rossetto, “Air forced convection through metal foams Experimental results and modeling,” International Journal of Heat and Mass Transfer, vol. 62, pp. 112-123, 2013.

[120] X. Chen, X. Xia, C. Sun, F. Wang and R. Liu, “Performance evaluation of a double-pipe heat exchanger with uniform and graded metal foams,” Heat and Mass Transfer, vol. 56, pp. 291-302, 2020.

Part 2

5. Overview of Work by ESR12

5.1 Need for Energy Storage Systems

The EU is aiming to stop the emission of greenhouse gas (GHG) by 2050 with an intermediate target for the reduction of at least 55% of GHG emissions by 2030 compared to the 1990 production [1]. These goals were set to stop the effects of climate change by limiting the global temperature rise to 1.5 °C. Renewable Energy Sources (RES) can play an important role in the current transition towards the use of less fossil fuels-based generators, without compromising energy security and the economic growth [2]. Despite the increase of the last years, energy production from RES needs to grow more rapidly. Currently, the main barriers that are preventing a deeper penetration of RES are their non-dispatchability, non-predictability and intermittency, which are making the grid management more challenging [3]. Being non-dispatchable means that the energy cannot be produced based on the demand needs, but it is dependent on the availability of natural sources, mainly wind and sun. For instance, during high availability of renewable power but low demand, the electric power needs to be transferred through transmission lines to locations where the demand is higher. However, the transportation of energy through long distances brings to higher losses. Moreover, there are some physical limitations to this since it is not possible to exceed the capacity of the transmission lines, as this would lead to congestions issues. In this case, the energy needs to be curtailed resulting in a waste of clean energy and in a loss of the plant revenue. This overgeneration risk can be visually identified in the so called “duck curve”, shown in Figure 5-1 [4]. This graph represents the net power demand of a typical spring day in California, showing a significant reduction over the years during the sunny hours of the day, mainly due to an increased installation of solar panels. Another issue that can be noticed from this graph is the increase of ramp needed during the evening hours, due to the combined effect of reduced power produced from sun and increased power demand, which poses additional challenges for conventional generators that need to quickly compensate for the non-availability of renewables sources.

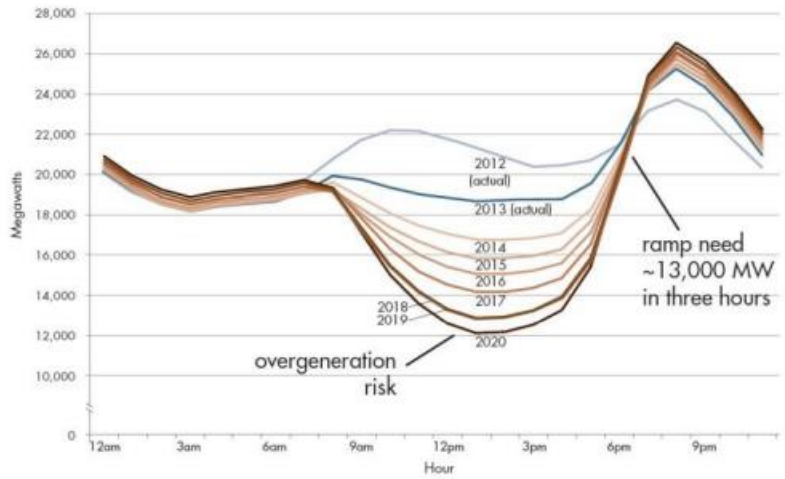

Figure 5-1: "The Duck Chart" [4]

Renewables are also difficult to predict as shown in Figure 5-2 which makes the energy planning more challenging [5].

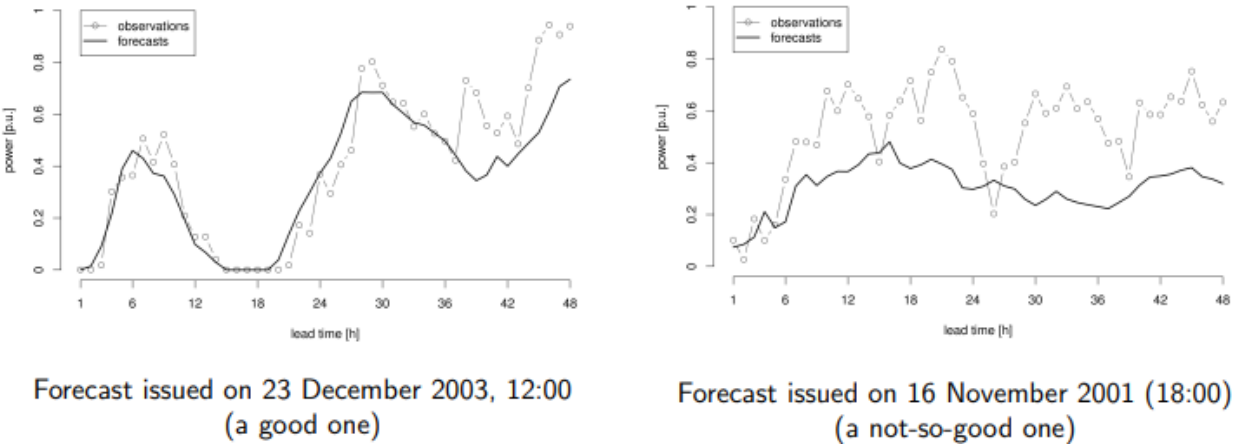

Figure 5-2: Example of wind power forecasts produced by an onshore wind farm in Northern Jutland, Denmark [5]

RES are also intermittent and this can lead to grid stability issues especially if there is a fast rate of change [5]. The intermittency is typical of electricity production from solar PV during partly cloudy weather. Figure 5-3 shows an example of power generation from solar panels for 3 different days. Day 1 is representative of a completely sunny day and therefore the energy production is smooth. However, day 2 and 3 represent the solar production with intermittency during cloudy days, where day 3 shows a higher variability of clouds during the day.

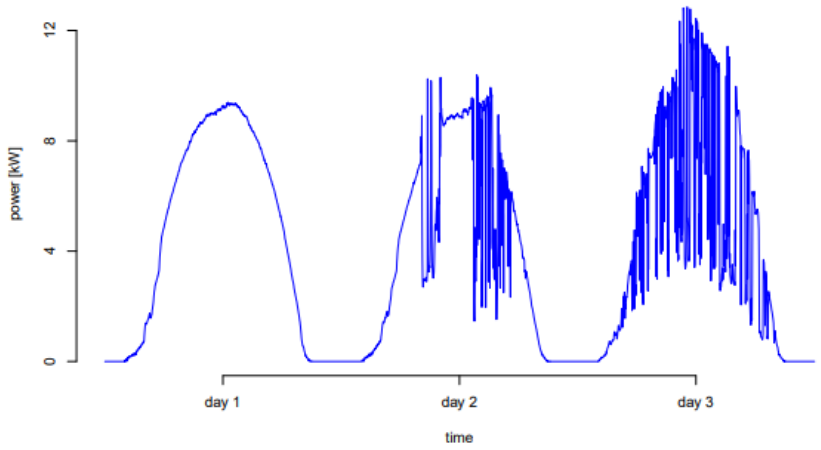

Figure 5-3: Example of intermittent power production from solar panels [5]

In a scenario with a low share of RES, these issues can be overcome by employing conventional generator that can compensate to these fluctuations ensuring that the energy supply is always matching the demand and providing ancillary services to maintain grid stability. However, the installation of RES has to increase and the production from carbon-based generators has to reduce. Alternative solutions should be investigated to reach higher flexibility. Energy storage systems (ESS) are devices able to store energy during excess of renewable production and release it later at a more convenient time. Therefore, ESS have the potential to reduce the mismatch between power production and demand, relieving the grid during the surplus of renewable production and supporting the reduction of fossil fuel utilization [6,7].

5.2 Distributed Generation with Micro Gas Turbines and Energy Storage Systems

The current energy scenario is not only changing in terms of energy mix but also on the structure of power plants layout which is moving from a hierarchical and supplier-centric structure towards a more decentralised and consumer-centric structure. This is because, the adoption of distributed generation systems can support a cleaner and more efficient energy production compared to traditional centralised power plants and can improve the exploitation of RES [8].

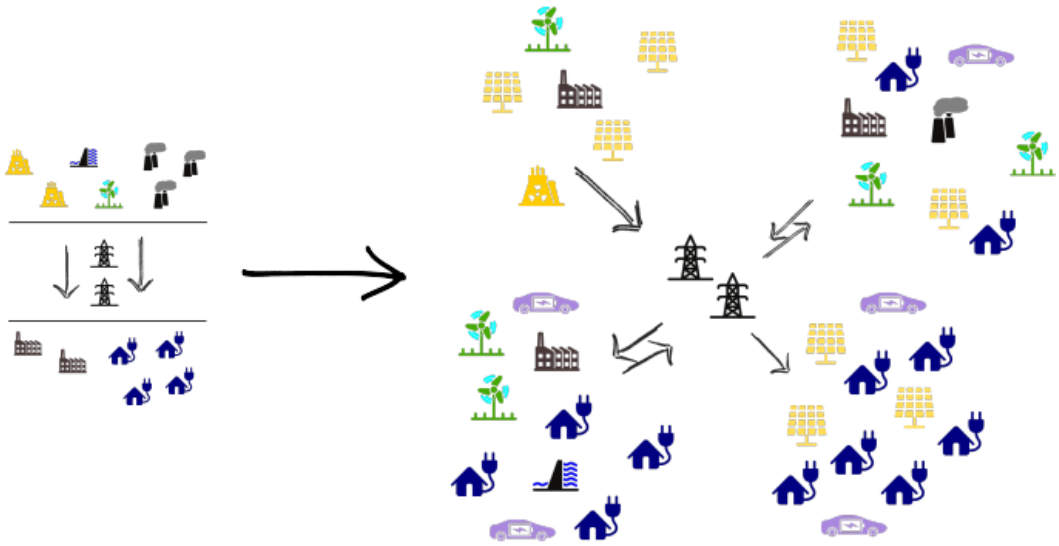

Figure 5-4: Change on the electrical power network from centralised to decentralised structure [9]

The use of small-scale generators close to the consumers can significantly improve energy conversion efficiencies due to the possibility to maximise local power production, reduce transportation and conversion losses and extensively employing cogeneration or trigeneration. Generally, distributed

generation systems can include different prime movers, characterised by different design and off-design behaviours, often including a significant share of unprogrammable green energy sources. Therefore, small size ESS represent an important asset to optimise the management of the different generators, reduce costs and match the energy demand of the end users [10]. In addition to ESS, also micro-GTs are interesting prime movers for distributed applications due to due to their high efficiency in combined heat and power (CHP) applications, low vibrations and noise levels, quick response, modularity and compact size [11–13]. Micro gas turbines are based on carbon-fuels, typically natural gas. However, in the future it could be possible to utilise them with green fuels such as hydrogen or alternative fuels obtained from hydrogen such as ammonia or methanol [14,15].

6. Energy Storage Systems Classification

Depending on the energy conversion process and storage medium, different storage systems are available, each of them with advantages and drawbacks depending on the considered application. The aim of this report is to describe the main energy storage technologies classified based on the conversion process mainly with a focus on technologies that can be coupled with micro gas turbines. Therefore, the considered energy storage systems are [6,16,17]:

- Mechanical energy storage systems
- Chemical energy storage systems
- Battery energy storage systems
- Thermal energy storage systems

6.1 Mechanical Energy Storage Systems

Mechanical energy storage systems convert the electricity in a form of mechanical energy such as pressurization or liquefaction of gas, kinetic or potential energy. The main examples of mechanical energy storage systems are flywheels, pumped hydro, and compressed air storage systems. This review will only focus on Compressed Air Energy Storage (CAES) systems due to their potential for small-size applications and possibility for the integration with micro-GT. The working principle of CAES is based on a Brayton cycle where compression and expansion are decoupled in time. An excess of renewable energy, typical of off-peak hours, can be used to power the compression system. The compressed air can be stored and then expanded in a turbine group to satisfy the electrical demand during peak hours [18]. While large size systems require to be placed closed to natural caverns due to the high volumes required for the air storage, in small CAES system air can be simply stored in artificial tanks, eliminating the dependency on geological formations. Compared to other storage solutions, such as batteries, small CAES systems are not susceptible to high temperatures, have lower capital cost and longer lifespan [19]. In addition, CAES systems are also suitable for cogenerative/trigenerative solutions as the thermal and cooling power can be extracted during the compression and expansion processes [20].

In conventional Diabatic-CAES (D-CAES) systems, the heat produced during compression is dissipated in the environment. Before the expansion, thermal energy is typically added through a combustion process [21,22]. To eliminate the dependency on the fuel, Adiabatic-CAES (A-CAES) solutions have been proposed by employing Thermal Energy Storage (TES) systems [23–25]. In this case, heat is not wasted but stored in the TES during the charging phase and it is released during the discharge. However, the increase in efficiency and the elimination of CO_2 emission are obtained at the expense of higher costs and plant complexity. Isothermal-CAES (I-CAES) systems have also been considered with the aim of eliminating the combustion process and the TES system at the same time, with potential benefits on both costs and efficiency [26]. Nearly isothermal compression and expansion can be obtained by using liquid pistons or hydraulic pumps/turbines, exploiting the higher thermal capacity of liquids. However, slow compression/expansions are required to leave sufficient time for the heat transfer exchange, which makes this not suitable for industrial applications. Faster processes can be obtained by introducing liquid or foam drops inside the air, but these solutions are not yet ready for a commercial

use [27]. An alternative option, namely second generation diabatic CAES, integrates the compression and storage systems with a standard micro gas turbine (mGT) [28–30]. In this solution, air can be compressed externally and then injected upstream of the mGT recuperator. The advantage of this system is that it can always satisfy the energy demand and at the same time the integration with the CAES system can bring benefits in terms of fuel savings. Typically, two different solutions are possible [29] as illustrated in Figure 6-1: 1) the compressed air can be directly injected at the exit of the micro-GT compressor or 2) the compressed air is pre-heated and expanded in an additional expander before being injected into the micro-GT.

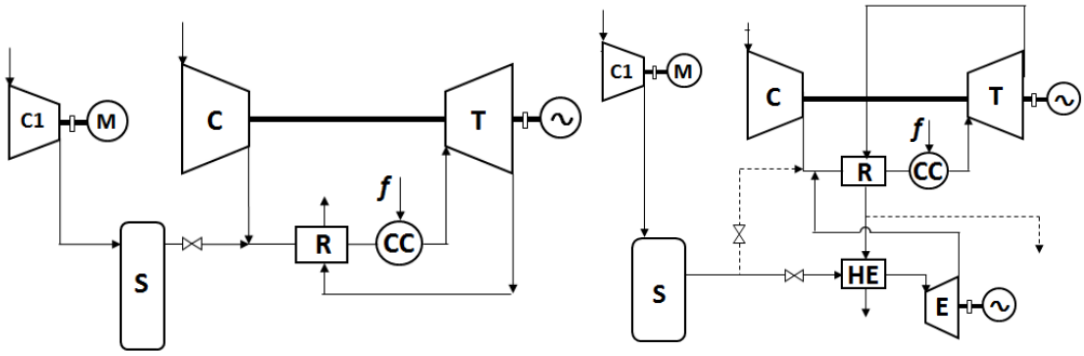

Figure 6-1: CAES Air Injection (left) and CAES Air Injection/Expander (right) [29]

6.2 Chemical Energy Storage Systems

Energy can be stored in the form of chemical energy. All the traditional carbon-based fuels, such as coal, gasoline, diesel, natural gas, liquefied petroleum gas (LPG), are a form of chemical storage. However, this review will focus on chemical storage that can be considered carbon-free. In particular, in this section chemical storage from hydrogen and ammonia production are considered due to their potentials for their use in micro-GTs. Chemical storage (also called, power-to-fuel) can give good flexibility and high energy storage capacity also for long term applications [31,32].
Hydrogen is an interesting option due its carbon-free formula and because it can be produced from water electrolysis, which can be powered from renewable energy overproduction. Various experimental studies have been conducted with blends containing low concentrations of H2 (around 10/15% in vol) in blend with natural gas to demonstrate the feasibility on commercial micro gas turbines [33,34]. However, the combustion of hydrogen in blend with natural gas at higher concentrations shows several issues because of the different combustion characteristics compared to conventional fossil fuels, for example higher LHV, higher reactivity, flame speed and burning velocity. Therefore, different research activities have been conducted with a focus on combustion CFD modelling to improve its efficiency, stability and reduce NOx emissions [15,35,36].

Hydrogen has also further limitations related to its low volumetric energy density, which makes its storage and distribution highly unpractical and expensive [37]. Consequently, alternative fuels with higher energy density should also be considered. In particular, ammonia can be synthetised from green H_2 and it is also carbon-free. It is easier and cheaper to store and transport due to an easier and less energy intense liquefaction and, at the same time, the procedures and standards for safely manage ammonia are already well-known by the experience of the chemical industry [14]. Ammonia combustion should also solve different issues related to the low LHV, low reactivity, high ignition energy and low laminar burning velocity [38]. Initial studies were mainly focusing on evaluating the effects of NH_3 in blends with CH_4 and H_2, where the latter can be produced from NH_3 dissociation [39]. A practical application has also been performed by researchers of the National Institute of Advanced Industrial Science and Technology (AIST) who were able to operate a 50 kW micro gas turbine fired

with ammonia-kerosene blends by means of a new diffusive bi-fuel combustor [40,41].

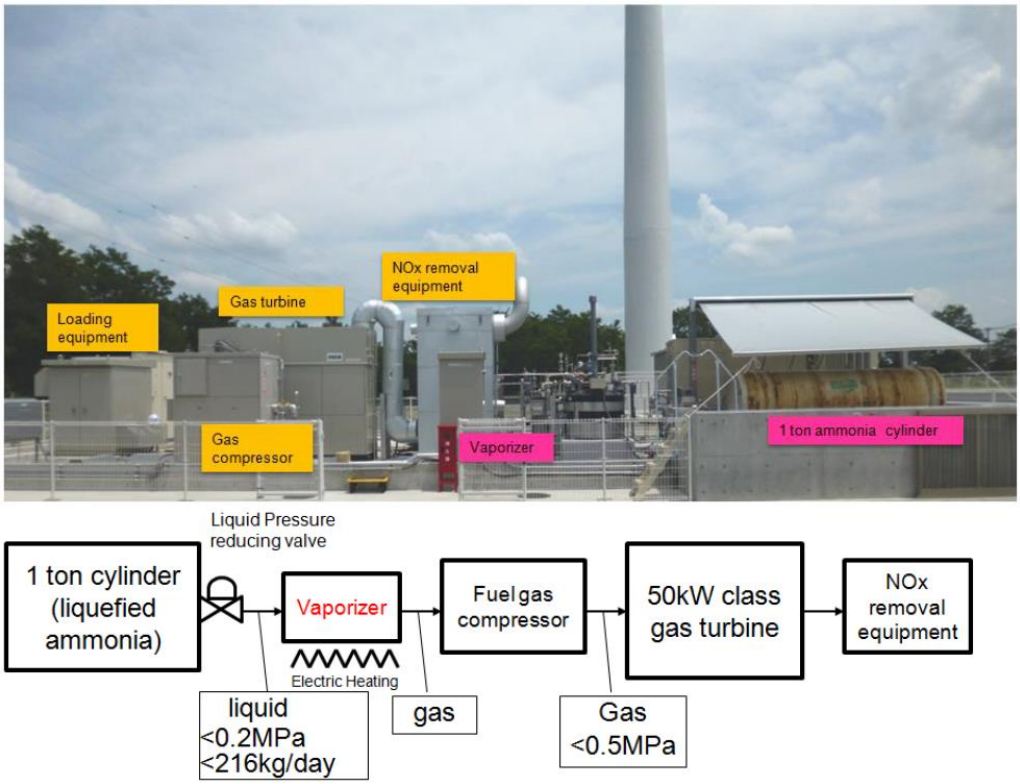

Figure 6-2: Facility of the ammonia micro-GT [40,41].

After that, they were also able to fire the micro gas turbine with pure ammonia thanks to a two staged rich-lean burner [42,43]. However, one of the limitations was the production of high NOx emissions which make essential the use of a selective catalytic reactor (SCR) for the reduction of NOx to acceptable limits.

6.3 Battery Energy Storage Systems

A battery can convert the chemical energy contained in its active materials, directly into electric energy by means of an electrochemical oxidation-reduction. Batteries are gaining a lot of interest due to their fast response time. The batteries used for stationary applications are deep cycle batteries with efficiencies around 70% to 80%, similarly to electric vehicles [44]. Due to the high cost and required capacity, the main applications for batteries in stationary applications are for short timescale due to the fast ramp rate, while for medium to long term timescales CAES systems and chemical energy storage have more potentials [17]. Batteries can be divided in 1) primary batteries or 2) secondary batteries. The first types are non-rechargeable and therefore not of interest for applications as energy storage systems. Instead, the second types are rechargeable and could be used for power production applications as they allow the current to pass through the circuit in the opposite direction of the current during discharge. Their electrolyte can be aqueous or nonaqueous, which are based on water and solvents respectively. Examples of batteries with aqueous electrolytes are Lead Acid, Nickel-Cadmium and Nickel–Metal Hydride, Batteries with nonaqueous Electrolytes include Lithium Ion, Lithium Metal, Metal Air and Sodium Sulphur [44].

6.4 Thermal Energy Storage Systems

Thermal energy storage systems can decouple the electrical and thermal production of micro-GTs. During high electrical power demand and low thermal demand, heat can be stored and used later at a more convenient time. This improves the overall efficiency of the system because the thermal energy

is not wasted. Thermal energy storage systems can be classified as it follows:

- *Sensible heat systems* [10]: in this case, the storage medium will increase or decrease its temperature during respectively the charging or discharging of the system. The sensible heat stored is proportional to the heat capacity of the medium, mass of the storage material and the temperature rise between initial and final states. The storage medium can be liquid (water, molten-salt or thermal-oil), solid (stone, concrete, metal or the ground), or liquid with solid filler material (molten-salt/stone). Their main advantages are the simplicity, ease of implementation and low costs.
- *Latent heat systems* [45] : differently from the sensible heat systems, latent heat storage are based on phase change materials (PCMs) and the charging and discharging of the system occur when the material undergoes a phase change (for example, melting, evaporating and crystallization), without temperature variation. PCMs have different advantages such as small temperature drops during heat recovery, high latent heat, stability, and non-toxicity, etc. Phase change can occur in different forms: solid–solid, solid–liquid, solid–gas, and liquid–gas.
- *Thermochemical heat storage systems* [46]: in this case, a reversible chemical reaction is used: the storage is charged during an endothermic reaction and discharged during an exothermic one. The thermochemical heat stored is dependent on the reaction enthalpy. Thermochemical heat storage systems store has the possibility to store both sensible heat and chemical energy, with the benefit of providing higher energy densities compared to latent and sensible. As downsides, their complexity and cost are a limit for the commercial applications.

References

[1] European Commission, 2050 long-term strategy, (n.d.). https://ec.europa.eu/clima/eu-action/climate-strategies-targets/2050-long-term-strategy_en.

[2] IEA, World Energy Model, IEA, Paris, (2021). https://www.iea.org/reports/world-energy-model.

[3] B.M.S. Hodge, H. Jain, C. Brancucci, G.S. Seo, M. Korpås, J. Kiviluoma, H. Holttinen, J.C. Smith, A. Orths, A. Estanqueiro, L. Söder, D. Flynn, T.K. Vrana, R.W. Kenyon, B. Kroposki, Addressing technical challenges in 100% variable inverter-based renewable energy power systems, Wiley Interdiscip. Rev. Energy Environ. 9 (2020) 1–19. https://doi.org/10.1002/wene.376.

[4] I. California, What the duck curve tells us about managing a green grid, (2020) 1–4.

[5] Pierre Pinson, Current challenges with renewables in electricity markets, (n.d.). http://pierrepinson.com/31761/Slides/31761lecture1p4.pdf.

[6] D.O. Akinyele, R.K. Rayudu, Review of energy storage technologies for sustainable power networks, Sustain. Energy Technol. Assessments. 8 (2014) 74–91. https://doi.org/10.1016/j.seta.2014.07.004.

[7] A. Bouakkaz, A.J.G. Mena, S. Haddad, M.L. Ferrari, Efficient energy scheduling considering cost reduction and energy saving in hybrid energy system with energy storage, J. Energy Storage. 33 (2021) 101887. https://doi.org/10.1016/j.est.2020.101887.

[8] M.F. Akorede, H. Hizam, E. Pouresmaeil, Distributed energy resources and benefits to the environment, Renew. Sustain. Energy Rev. 14 (2010) 724–734. https://doi.org/10.1016/j.rser.2009.10.025.

[9] Pierre Pinson, D. Prices, Fundamental of electricity markets - historiacal perspective, (n.d.). http://pierrepinson.com/31761/Slides/31761lecture1p1.pdf.

[10] M.L. Ferrari, A. Cuneo, M. Pascenti, A. Traverso, Real-time state of charge estimation in thermal storage vessels applied to a smart polygeneration grid, Appl. Energy. 206 (2017) 90–100. https://doi.org/10.1016/j.apenergy.2017.08.062.

[11] P.A. Pilavachi, Mini- and micro-gas turbines for combined heat and power, Appl. Therm. Eng. 22 (2002) 2003–2014. https://doi.org/10.1016/S1359-4311(02)00132-1.

[12] L. Magistri, P. Costamagma, A.F. Massardo, C. Rodgers, C.F. MacDonald, A hybrid system based on a personal turbine (5 kW) and a solid oxide fuel cell stack: A flexible and high efficiency energy concept for the distributed power market, J. Eng. Gas Turbines Power. 124 (2002) 850–857. https://doi.org/10.1115/1.1473825.

[13] A. Giugno, L. Mantelli, A. Cuneo, A. Traverso, Performance analysis of a fuel cell hybrid system subject to technological uncertainties, Appl. Energy. 279 (2020) 115785. https://doi.org/10.1016/j.apenergy.2020.115785.

[14] A. Valera-Medina, H. Xiao, M. Owen-Jones, W.I.F. David, P.J. Bowen, Ammonia for power, Prog. Energy Combust. Sci. 69 (2018) 63–102. https://doi.org/10.1016/j.pecs.2018.07.001.

[15] A. Cappelletti, F. Martelli, E. Bianchi, E. Trifoni, Numerical redesign of 100kW MGT combustor for 100% H2 fueling, Energy Procedia. 45 (2014) 1412–1421. https://doi.org/10.1016/j.egypro.2014.01.148.

[16] M. Faisal, M.A. Hannan, P.J. Ker, A. Hussain, M. Bin Mansor, F. Blaabjerg, Review of energy storage system technologies in microgrid applications: Issues and challenges, IEEE Access. 6 (2018) 35143–35164. https://doi.org/10.1109/ACCESS.2018.2841407.

[17] A.Z. AL Shaqsi, K. Sopian, A. Al-Hinai, Review of energy storage services, applications, limitations, and benefits, Energy Reports. 6 (2020) 288–306. https://doi.org/10.1016/j.egyr.2020.07.028.

[18] J. Wang, K. Lu, L. Ma, J. Wang, M. Dooner, S. Miao, J. Li, D. Wang, Overview of compressed air energy storage and technology development, Energies. 10 (2017). https://doi.org/10.3390/en10070991.

[19] M. Heidari, D. Parra, M.K. Patel, Physical design, techno-economic analysis and optimization of distributed compressed air energy storage for renewable energy integration, J. Energy Storage. 35 (2021) 102268. https://doi.org/10.1016/j.est.2021.102268.

[20] A.L. Facci, D. Sánchez, E. Jannelli, S. Ubertini, Trigenerative micro compressed air energy storage: Concept and thermodynamic assessment, Appl. Energy. 158 (2015) 243–254. https://doi.org/10.1016/j.apenergy.2015.08.026.

[21] S. Briola, P. Di Marco, R. Gabbrielli, J. Riccardi, A novel mathematical model for the performance assessment of diabatic compressed air energy storage systems including the turbomachinery characteristic curves, Appl. Energy. 178 (2016) 758–772. https://doi.org/10.1016/j.apenergy.2016.06.091.

[22] E. Yao, H. Wang, L. Wang, G. Xi, F. Maréchal, Thermo-economic optimization of a combined cooling, heating and power system based on small-scale compressed air energy storage, Energy Convers. Manag. 118 (2016) 377–386. https://doi.org/10.1016/j.enconman.2016.03.087.

[23] M. Minutillo, A. Lubrano Lavadera, E. Jannelli, Assessment of design and operating parameters for a small compressed air energy storage system integrated with a stand-alone renewable power plant, J. Energy Storage. 4 (2015) 135–144. https://doi.org/10.1016/j.est.2015.10.002.

[24] C. Mcculloch, M. Ghavami, J. Al Zaili, A. Sayma, Design and Analysis of an Adiabatic Micro-Compressed Air Energy Storage System, (2020) 1–9.

[25] P. Zhao, M. Wang, J. Wang, Y. Dai, A preliminary dynamic behaviors analysis of a hybrid energy storage system based on adiabatic compressed air energy storage and flywheel energy storage system for wind power application, Energy. 84 (2015) 825–839. https://doi.org/10.1016/j.energy.2015.03.067.

[26] E.M. Gouda, Y. Fan, M. Benaouicha, T. Neu, L. Luo, Review on Liquid Piston technology for compressed air energy storage, J. Energy Storage. 43 (2021) 103111. https://doi.org/10.1016/j.est.2021.103111.

[27] H. Chen, Y. hang Peng, Y. ling Wang, J. Zhang, Thermodynamic analysis of an open type isothermal compressed air energy storage system based on hydraulic pump/turbine and spray cooling, Energy Convers. Manag. 204 (2020) 112293. https://doi.org/10.1016/j.enconman.2019.112293.

[28] G.L. Arnulfi, G. Croce, Compressed air energy storage for a small size standalone plant powered by a solar power unit and a gas turbine, Proc. ASME Turbo Expo. 5 (2020) 1–10. https://doi.org/10.1115/GT2020-14631.

[29] C. Salvini, Performance Analysis of Small Size Compressed Air Energy Storage Systems for Power Augmentation: Air Injection and Air Injection/Expander Schemes, Heat Transf. Eng. 39 (2018) 304–315. https://doi.org/10.1080/01457632.2017.1295746.

[30] C. Salvini, Techno-economic analysis of small size second generation CAES system, Energy Procedia. 82 (2015) 782–788. https://doi.org/10.1016/j.egypro.2015.11.812.

[31] M. Rivarolo, D. Rattazzi, L. Magistri, A.F. Massardo, Multi-criteria comparison of power generation and fuel storage solutions for maritime application, Energy Convers. Manag. 244 (2021) 114506. https://doi.org/10.1016/j.enconman.2021.114506.

[32] M. Minutillo, A. Perna, A. Sorce, Green hydrogen production plants via biogas steam and autothermal reforming processes: energy and exergy analyses, Appl. Energy. 277 (2020) 115452. https://doi.org/10.1016/j.apenergy.2020.115452.

[33] R. Calabria, F. Chiariello, P. Massoli, F. Reale, Part load behavior of a micro gas turbine FED with different fuels, Proc. ASME Turbo Expo 2014. 1B (2014) 1–11. https://doi.org/10.1115/GT2014-26631.

[34] M. du Toit, N. Engelbrecht, S.P. Oelofse, D. Bessarabov, Performance evaluation and emissions reduction of a micro gas turbine via the co-combustion of H2/CH4/CO2 fuel blends, Sustain. Energy Technol. Assessments. 39 (2020) 100718. https://doi.org/10.1016/j.seta.2020.100718.

[35] C. Devriese, W. Pennings, H. de Reuver, R. Bastiaans, W. De Paepe, The Preliminary CFD Design of a Compressor and Combustor System Towards a 100 kW Hydrogen Fuelled Micro Gas Turbine, Proc. ASME Turbo Expo 2019. (2019) 1–10. https://doi.org/10.1115/GT2019-91342.

[36] R. Tuccillo, M.C. Cameretti, R. De Robbio, F. Reale, F. Chiariello, Methane-Hydrogen Blends in Micro Gas Turbines: Comparison of Different Combustor Concepts, Proc. ASME Turbo Expo 2019. (2019) 1–13. https://doi.org/10.1115/GT2019-90229.

[37] J.O. Abe, A.P.I. Popoola, E. Ajenifuja, O.M. Popoola, Hydrogen energy, economy and storage: Review and recommendation, Int. J. Hydrogen Energy. 44 (2019) 15072–15086. https://doi.org/10.1016/j.ijhydene.2019.04.068.

[38] H. Kobayashi, A. Hayakawa, K.D.K.A. Somarathne, E.C. Okafor, Science and technology of ammonia combustion, Proc. Combust. Inst. 37. (2019) 109–133. https://doi.org/10.1016/j.proci.2018.09.029.

[39] A. Valera-Medina, S. Morris, J. Runyon, D.G. Pugh, R. Marsh, P. Beasley, T. Hughes, Ammonia, Methane and Hydrogen for Gas Turbines, in: Energy Procedia 75, 2015: pp. 118–123. https://doi.org/10.1016/j.egypro.2015.07.205.

[40] N. Iki, O. Kurata, T. Matsunuma, T. Inoue, M. Suzuki, T. Tsujimura, H. Furutani, Micro Gas Turbine Operation with Kerosene and Ammonia, 11th Annu. NH3 Fuel Conf. (2014) 1–22.

[41] N. Iki, O. Kurata, T. Matsunuma, T. Inoue, T. Tsujimura, H. Furutani, H. Kobayashi, A. Hayakawa, A. Ichikawa, Y. Arakawa, Micro gas turbine firing ammonia, in: Proc. ASME Turbo Expo 2016, 2016: pp. 1–6. https://doi.org/https://doi.org/10.1115/GT2016-56954.

[42] O. Kurata, N. Iki, T. Inoue, T. Fujitani, Y. Fan, T. Matsunuma, T. Tsujimura, H. Furutani, M. Kawano, K. Arai, E.C. Okafor, A. Hayakawa, H. Kobayashi, Pure Ammonia Combustion Micro Gas Turbine System, (2019).

[43] O. Kurata, N. Iki, Y. Fan, T. Matsunuma, T. Inoue, T. Tsujimura, H. Furutani, M. Kawano, K. Arai, E.C. Okafor, A. Hayakawa, H. Kobayashi, Start-up process of 50kW-class gas turbine firing ammonia gas, in: Proc. ASME Turbo Expo 2021, 2021: pp. 1–7. https://doi.org/https://doi.org/10.1115/GT2021-59448.

[44] K.C. Divya, J. Østergaard, Battery energy storage technology for power systems-An overview, Electr. Power Syst. Res. 79 (2009) 511–520. https://doi.org/10.1016/j.epsr.2008.09.017.

[45] W. Liu, Y. Bie, T. Xu, A. Cichon, G. Królczyk, Z. Li, Heat transfer enhancement of latent heat thermal energy storage in solar heating system: A state-of-the-art review, J. Energy Storage. 46 (2022). https://doi.org/10.1016/j.est.2021.103727.

[46] X. Zhou, M. Mahmood, J. Chen, T. Yang, G. Xiao, M.L. Ferrari, Validated model of thermochemical energy storage based on cobalt oxides, Appl. Therm. Eng. 159 (2019) 113965. https://doi.org/10.1016/j.applthermaleng.2019.113965.

7. MGT Model Validated with Experimental Results (Validation of a T100 Transient Model with Injection of Compressed Air)

Experimental activities were conducted at the Innovative Energy System Laboratory (IES Lab) in the Savona Campus of the University of Genoa to validate a transient model of a Turbec T100 micro gas turbine when injecting compressed air upstream of the recuperator. The injection of air is used to simulate the interaction with a Compressed Air Energy Storage (CAES) system in the moment where air is discharged from a tank into the mGT. The interest on CAES systems is related to the additional flexibility that could be added to the system when coupled with intermittent and non-dispatchable renewable energy sources. If the renewable production exceeds the demand, the surplus of energy could be used to compress air. The air can be stored and injected later into a micro gas turbine when the renewable production is lower than the demand. This brings befits in terms of increased local consumptions, higher renewable exploitation and fuel consumption reduction.

The operation of the mGT with augmented mass flow, such as in the case of air injection, can increase the risk of compressor surge since the compressor and turbine operating matching point will move closer to the surge line. Compressor surge is a dangerous condition consisting of mass flow and pressure fluctuations. Transient models are interesting tools that can be used to predict if the compressor is

working safely in all the operating conditions, with the possibility to analyse different transient manoeuvres that cannot be modelled with simple steady-state off-design models. The transient model was developed with the software TRANSEO, which consists of a library of modular components to be used in the MATLAB/Simulink environment, developed by the Thermochemical Power Group of the University of Genoa.

Initial studies were already carried out on a validated TRANSEO model of a T100. However, the model was validated only analysing typical transient manoeuvres such as power increase and decrease steps in normal operation (without injection of air) and it was validated based on a different T100 available at the Vrije Universiteit Brussel [1]. Therefore, there is the need to validate the model also during air injection operating by employing an mGTs available at the University of Genoa.

7.1 Test Set-Up

The experimental activities were conducted on a Turbec T100, a compact mGT for CHP applications based on a recuperated cycle. The nominal electrical and thermal power outputs are 100 kWe and 165 kWth, the electrical efficiency is 30% and the overall cogeneration efficiency is 80% [2]. All the main nominal technical characteristics are summarized in Table 2.

Table 2: T100 NOMINAL SPECIFICATIONS

Electrical power	100	kW
Thermal power	165	kW
Electrical efficiency	0.3	-
Overall cogeneration efficiency	0.8	-
Pressure ratio	4.5	-
Rotational speed	70000	rpm
Turbine outlet temperature	918	K

The experimental facility has been previously described in different publications [3–5]. The main purpose of this facility was to model a T100 connected with a fuel cell emulator. For this reason, the micro gas turbine was connected with a high temperature volume with a new set of pipes for the physical emulation (Figure 3). However, in this specific case, it is of interest to test only the T100 and therefore the valves connecting the volume (VC, VR and VO) were closed. Although the T100 is equipped with standard probes for control and diagnostic, additional sensors were added to measure a higher number of properties. Table 3 summarises just the parameters used for the validation.

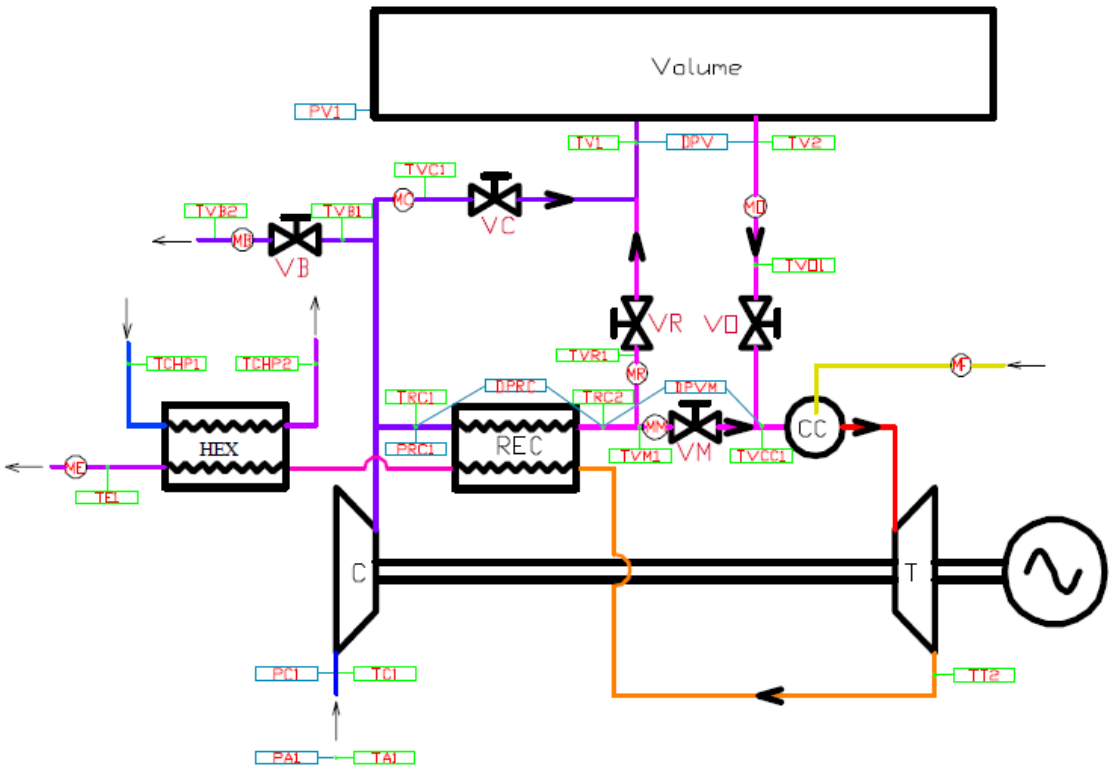

Figure 3: PLANT LAYOUT AND INSTRUMENTATION

The compressed air was injected upstream of the recuperator as in the TRANSEO model. The compressed air was obtained with a compressor able to elaborate a maximum mass flow of 30 g/s. The air was injected at constant power first with a step from 0 g/s to 15 g/s and then with a step from 15 g/s to 30 g/s (maximum compressor delivery mass flow). The air was injected imposing a constant electrical power (40 kW and 60 kW) for the mGT and, after that, imposing the maximum load.

Table 3: List of measured parameters used for the validation

Name	**Description**
TRC1	Recuperator inlet temperature cold side
TRC2	Recuperator outlet temperature cold side
TVCC1	Combustor inlet temperature
TOT	Turbine outlet temperature
TRE	Recuperator outlet temperature hot side
PRC1	Recuperator inlet pressure cold side
PRC	Recuperator outlet pressure cold side
PVM	Combustor inlet pressure
N	Rotational speed
MM	Main line mass flow

The summary of the operations during the experiments is listed below and can be visually identified in Figure 4:

1) Steady-state condition reached at 40 kW and 0 g/s of injected air
2) Step from 0 g/s to 15 g/s of injected air at 40 kW
3) Step from 15 g/s to 30 g/s of injected air at 40 kW
4) Step from 30 g/s to 15 g/s of injected air at 40 kW
5) Step from 15 g/s to 0 g/s of injected air at 40 kW
6) Power step from 40 kW to 60 kW

7) Step from 0 g/s to 15 g/s of injected air at 60 kW
8) Step from 15 g/s to 30 g/s of injected air at 60 kW
9) Step from 30 g/s to 15 g/s of injected air at 60 kW
10) Step from 15 g/s to 0 g/s of injected air at 60 kW
11) Power step from 60 kW to the maximum allowed power output (around 72.3 kW)
12) Step from 0 g/s to 15 g/s of injected air at the maximum allowed power output (because of the air injection a higher power output is reached at around 75 kW)
13) Step from 15 g/s to 30 g/s of injected air at the maximum allowed power output (because of the air injection a higher power output is reached at around 78 kW)

The T100 maximum electrical power output was below the nominal value (100 kW) because the tests were carried out with an ambient temperature in the 298 K–300 K range which is higher than the nominal ambient temperature (288 K) and the additional pipes od the system produced higher pressure losses (it is a typical and well-known limitation of the used facility).

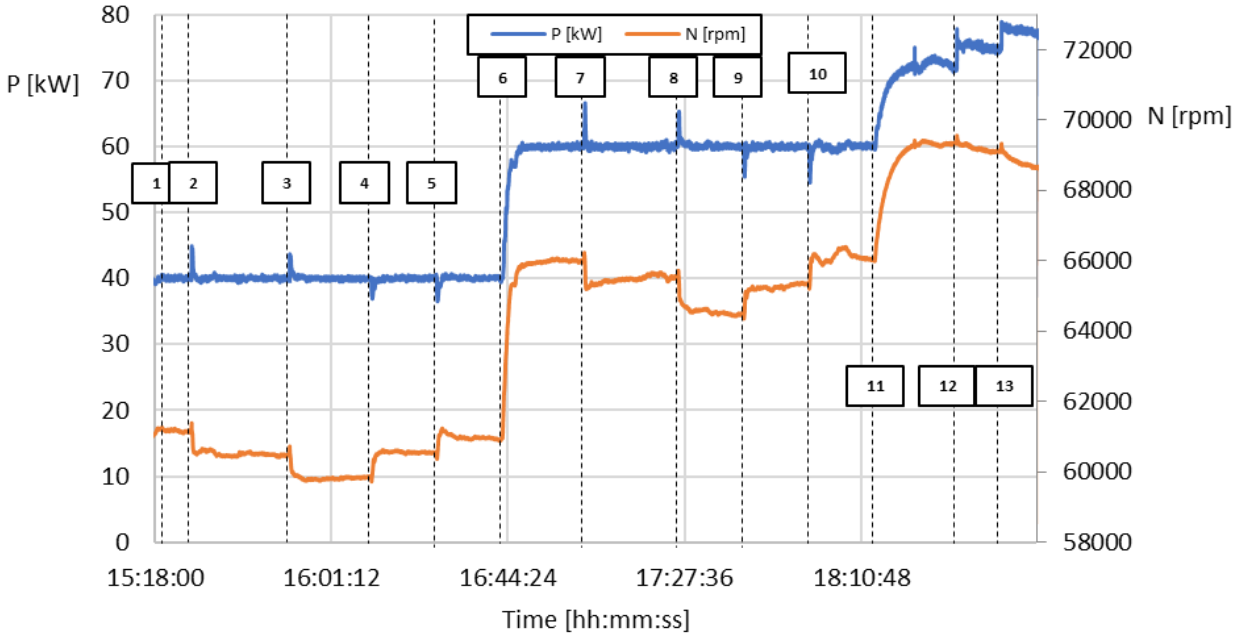

Figure 4: NET POWER OUTPUT AND ROTATIONAL SPEED FROM TESTS

7.2 TRANSEO Model Description

The software TRANSEO consists of a library of modular components, whose component and its interconnecting logic have already been validated in previous publications [6,7].

Regarding the interconnecting approach, the so-called "mass continuity" logic was used. In this way, each component is linked to the adjacent ones by receiving the information of the mass flow rate from either the upstream or downstream component and by sending in the opposite direction the pressure information. This method is able to provide a good compromise between calculation accuracy and computational time [1].

Regarding the modelling of the components, the compressor, turbine and combustor are modelled according to a "lumped-volume" approach. The component thermodynamic properties are obtained with a superposition of the effects which (i) calculates the steady-state off-design properties and then (ii) determines the dynamic behaviour by modelling the component as a duct of equivalent cross-sectional area and length. At each time step, the equations that are solved are the continuity,

momentum and energy equations. The steady-state calculation depends on the considered component. For the compressor and turbine, 0-D non-dimensional characteristic maps are used. For the combustor the energy equation is solved by taking into account of the combustion efficiency.

In the case of the recuperator a "quasi-2D approach" is used where the component is divided into four main parts representing the hot and cold flow passages, the internal matrix and the external vessel. Each main part is then longitudinally discretized into 10 elements to improve the calculation accuracy of the dynamic energy and heat transfer equations that are solved through a finite difference mathematical scheme.

The model also includes the T100 control system, which controls the electrical power output with a feedforward and a slow PI technique and, at the same time, keeps the Turbine Outlet Temperature (TOT) equal to 918 K by means of a fast PID controller which manages the fuel valve opening. The TRANSEO model of the T100 can be seen in Figure 5. The air was injected upstream of the recuperator in the "plenum" component.

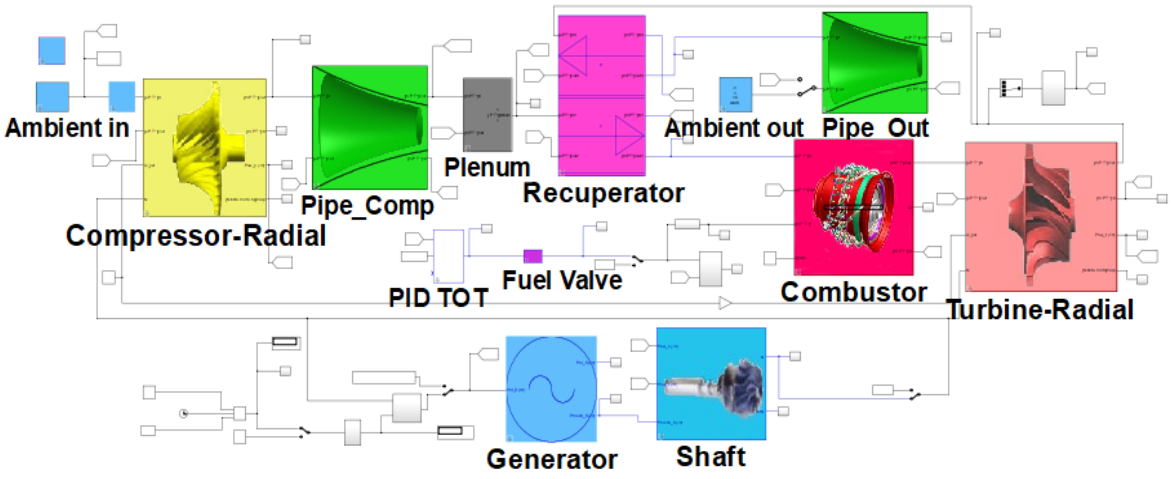

Figure 5: Transient model of the T100 in TRANSEO

7.3 Model Validation

The model was validated for both the steady-state and dynamic conditions. For simplicity, for the steady-state operations, the comparison between measured and calculated values is shown (Figure 6) only for of the cases without air injection. For completeness, Figure 7 summarizes the percentage errors for all the considered cases (no injection, injection of 15 g/s and injection of 30 g/s). While for the cases without air injection the comparison was performed at P=40 kW, 60 kW and 72.3 kW, for the cases with air injection the comparison was performed only at P=40 kW, 60 kW. This is because the developed TRANSEO model is yet not able to determine the maximum power output since at the moment the power output of the mGT is an input value for the model that has to be specified. The addition of this capability within the model will be included in future activities. The comparisons against steady-state results of Figure 7 shows a good matching with errors all below 1.5%, except from the TRE and TRC2 where the error is higher but still below 2.2%.

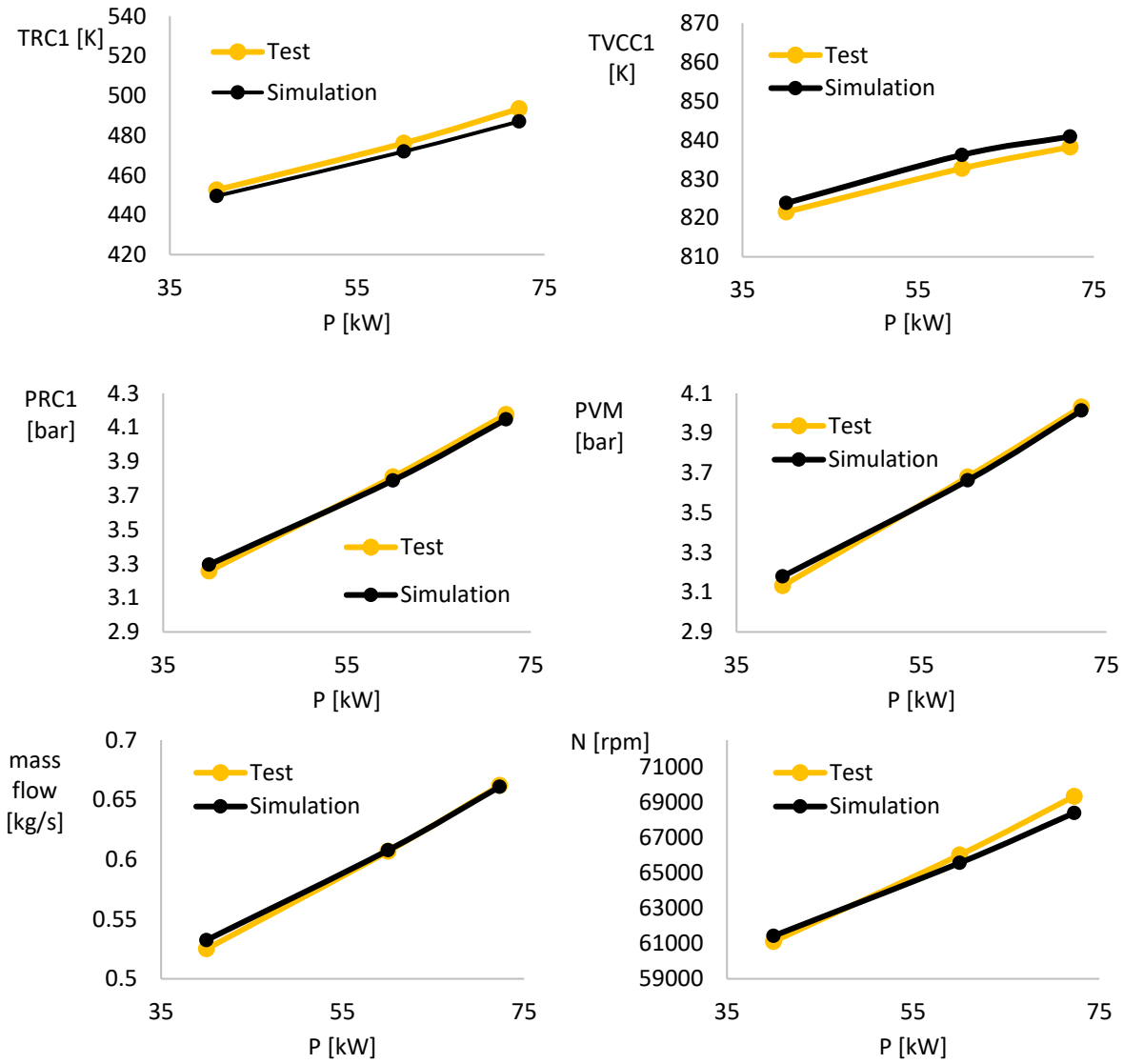

Figure 6: COMPARISON BETWEEN THE STEADY-STATE EXPERIMENTAL AND SIMULATED RESULTS FOR THE MAIN CYCLE PARAMETERS

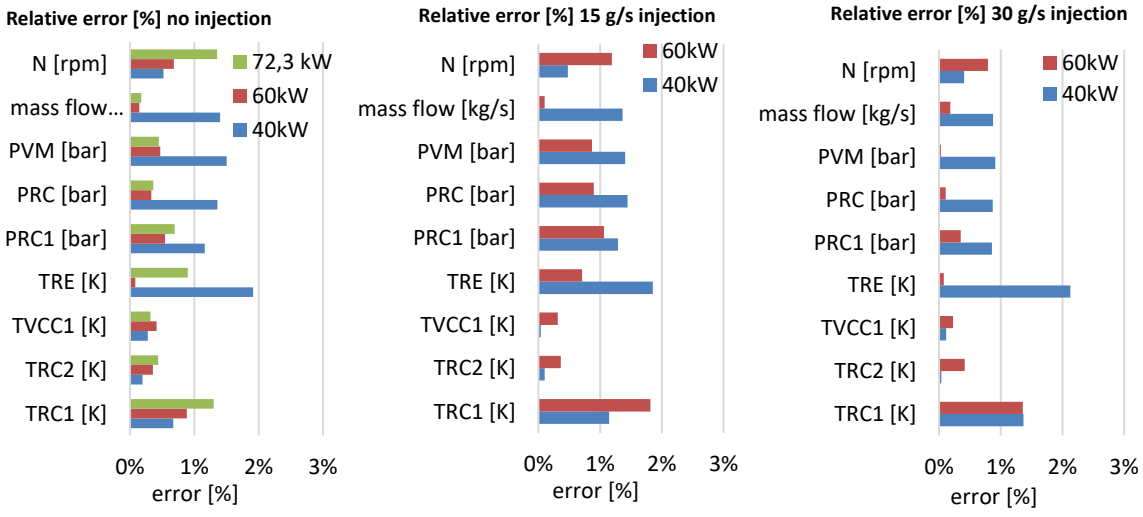

Figure 7: PERCENTAGE ERRORS OF THE RESULTS OF THE MODEL RELATIVE TO THE

EXPERIMENTAL DATA FOR THE MAIN CYCLE PARAMETERS

Following the steady-state validation of the T100 with injection of air, the transient behaviour was also validated. The dynamic behaviour of the model was also validated considering the case of a step change of injected air from 0 g/s to 15 g/s at constant P = 60 kW. Also in this case, some of the main performance parameters were compared against the measured experimental data providing a good agreement during the transient operation.

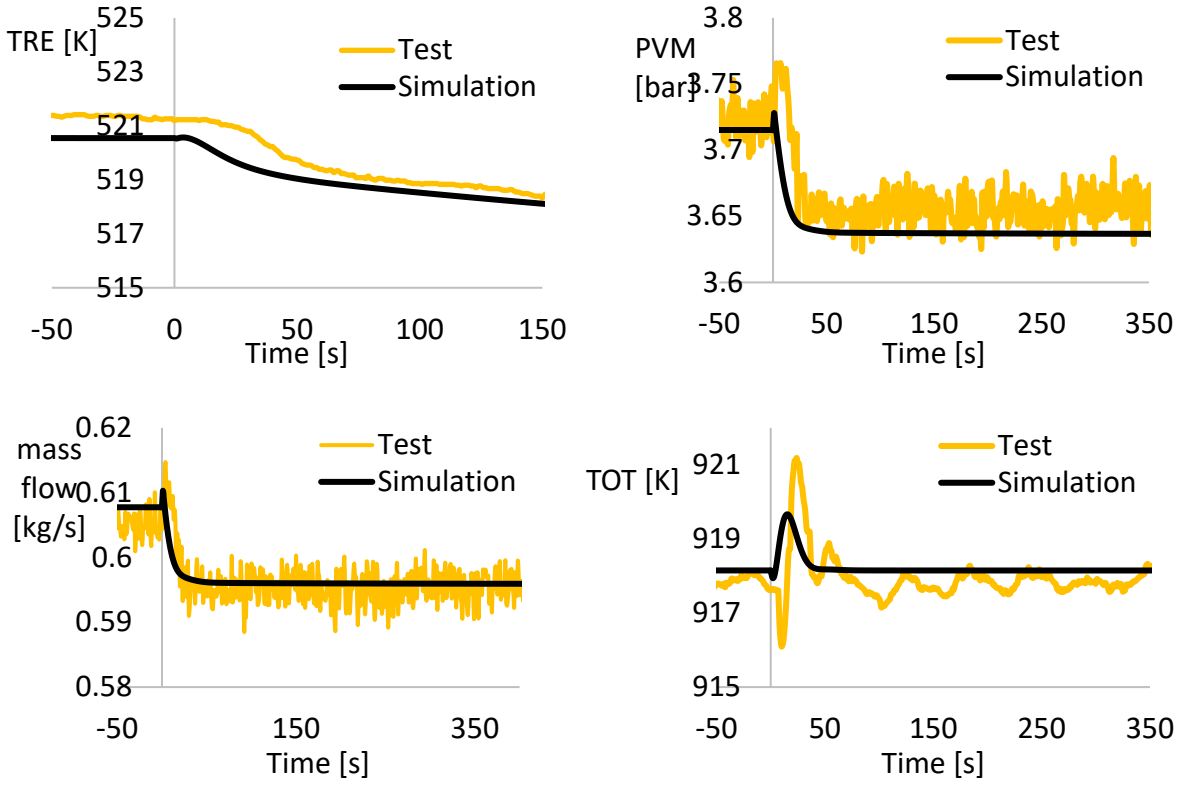

Figure 8: COMPARISON BETWEEN THE DYNAMIC EXPERIMENTAL AND SIMULATED RESULTS FOR THE MAIN CYCLE PARAMETERS AT CONSTANT P = 60 kW WITH INJECTION OF 15 g/s

8. Conclusions

Experimental activities were conducted on a T100 imposing a constant power of 40 kW, 60 kW and maximum load and injecting different amounts of compressed air (0 g/s, 15 g/s, 30 g/s) to simulate the effect of the discharge of a CAES system on the mGT. The TRANSEO tool was successfully validated against steady-state experimental data both in normal operation and with air injection. The obtained steady-state errors for the main cycle parameters were below 1.5 % except from the TRE and TRC2 where the error was higher but still below 2.2%. In addition, also the model results for transient operation with air injection showed a good agreement with the experimental data.

References

[1] M. Montero Carrero, M.L. Ferrari, W. De Paepe, A. Parente, S. Bram, F. Contino, Transient simulations of a T100 micro gas turbine converted into a micro humid air turbine, Proc. ASME Turbo Expo 2015. (2015) 1–9. https://doi.org/https://doi.org/10.1115/GT2015-43277.

[2] Ansaldo Energia, AE-T100 Micro Turbine Natural Gas, (2016) 2. https://www.atetsrl.it/Content/Atet/Images/Partner/Ansaldo/allegato (4).pdf.

[3] M.L. Ferrari, M. Pascenti, L. Magistri, A.F. Massardo, Hybrid system test rig: Start-up and shutdown physical emulation, J. Fuel Cell Sci. Technol. 7 (2010) 0210051–0210057. https://doi.org/10.1115/1.3176663.

[4] M. Pascenti, L. Magistri, M.L. Ferrari, A.F. Massardo, Micro gas turbine based test RIG for hybrid system emulation, Proc. ASME Turbo Expo. 3 (2007) 7–15. https://doi.org/10.1115/GT2007-27075.

[5] M.L. Ferrari, M. Pascenti, R. Bertone, L. Magistri, Hybrid simulation facility based on commercial 100 kWe micro gas turbine, J. Fuel Cell Sci. Technol. 6 (2009) 0310081–0310088. https://doi.org/10.1115/1.3006200.

[6] A. Traverso, F. Calzolari, A. Massardo, Transient analysis of and control system for advanced cycles based on micro gas turbine technology, J. Eng. Gas Turbines Power. 127 (2005) 340–347. https://doi.org/10.1115/1.1839918.

[7] A. Traverso, A.F. Massardo, R. Scarpellini, Externally Fired micro-Gas Turbine: Modelling and experimental performance, Appl. Therm. Eng. 26 (2006) 1935–1941. https://doi.org/10.1016/j.applthermaleng.2006.01.013.